Stockholm University

Master Thesis

Degree Project in
Geology 30 hp

Evaluation of deep geothermal energy in Sweden from literature review and eight case studies

Elof Tehler

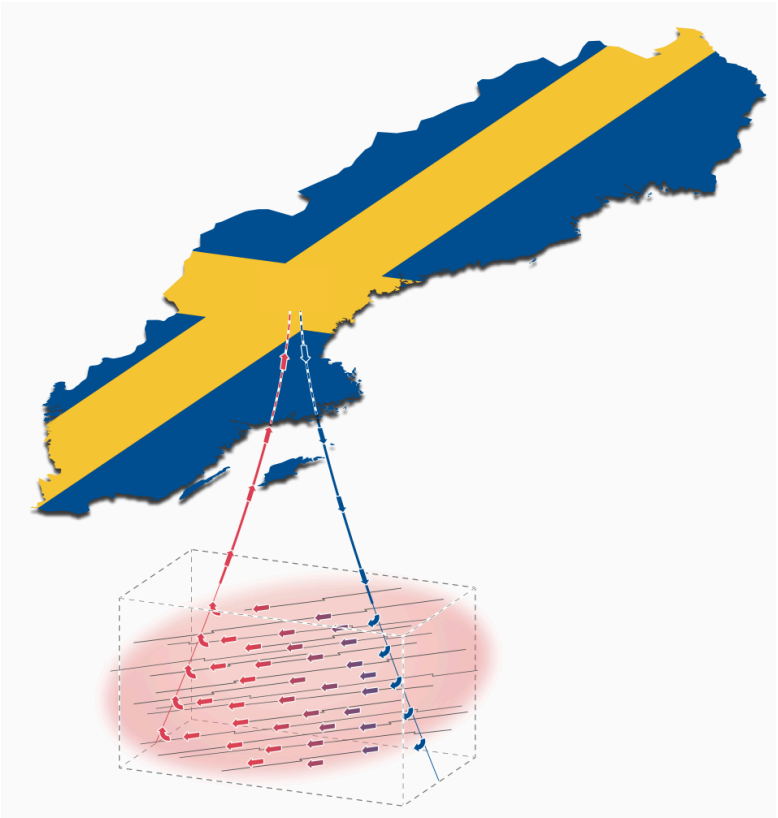

Stockholm 2023

Department of Geological Sciences
Stockholm University
SE-106 91 Stockholm

Table of content

Abstract

The demand for new renewable energy sources is increasing, and so does the investment in Enhanced Geothermal Systems (EGS) where hot, impermeable rocks are stimulated to develop artificial reservoirs for use in heat exchange. EGS is usually tested in areas with high geothermal gradients and low permeability to generate electricity. Recently, low gradients and low permeability have been tested for EGS as a heat source for the district heating network in Espoo, Finland. The project was terminated in 2022, achieving insufficient fluid flow between the injection and production wells at 6 km depth in the crystalline Fennoscandian Shield. In this review, the six deepest EGS projects in crystalline rocks are summarized and evaluated. The main geological and operational parameters to maximize chances of developing a similar EGS project in Sweden are assessed. Despite many uncertainties, the chance to develop the first deep geothermal district heating plant in Sweden is considered promising.

Introduction

Sweden has three climate zones according to the Köppen-Geiger Climate Classification: temperate in the south, boreal in the north, and polar in the mountains (Figure 1A). Due to this cold climate, approximately 22 % the total energy consumption in Sweden is allocated to heating of property (Energimyndigheten, 2023). Approximately half of this heating comes from district heating (Energimyndigheten, 2023). The district heating systems in Swedish cities and villages are relatively well-developed and the country has more than 500 systems with an increasing market share, replacing the oil from the pre-1970s (Figure 1C) (Werner, 2017). District heating is usually considered as the most environmental friendly alternative for heating due its fundamental idea to use local fuel or heat recourses that would otherwise be wasted (Werner, 2017). On average, the district heating production in Sweden comes mostly from combustion of biofuels, waste and fossil fuels (Figure 1B). This combustion is solely responsible for 8% of the total greenhouse gas emissions in Sweden (Olsson et al., 2015). Despite modern filtering incineration systems, the combustion releases small

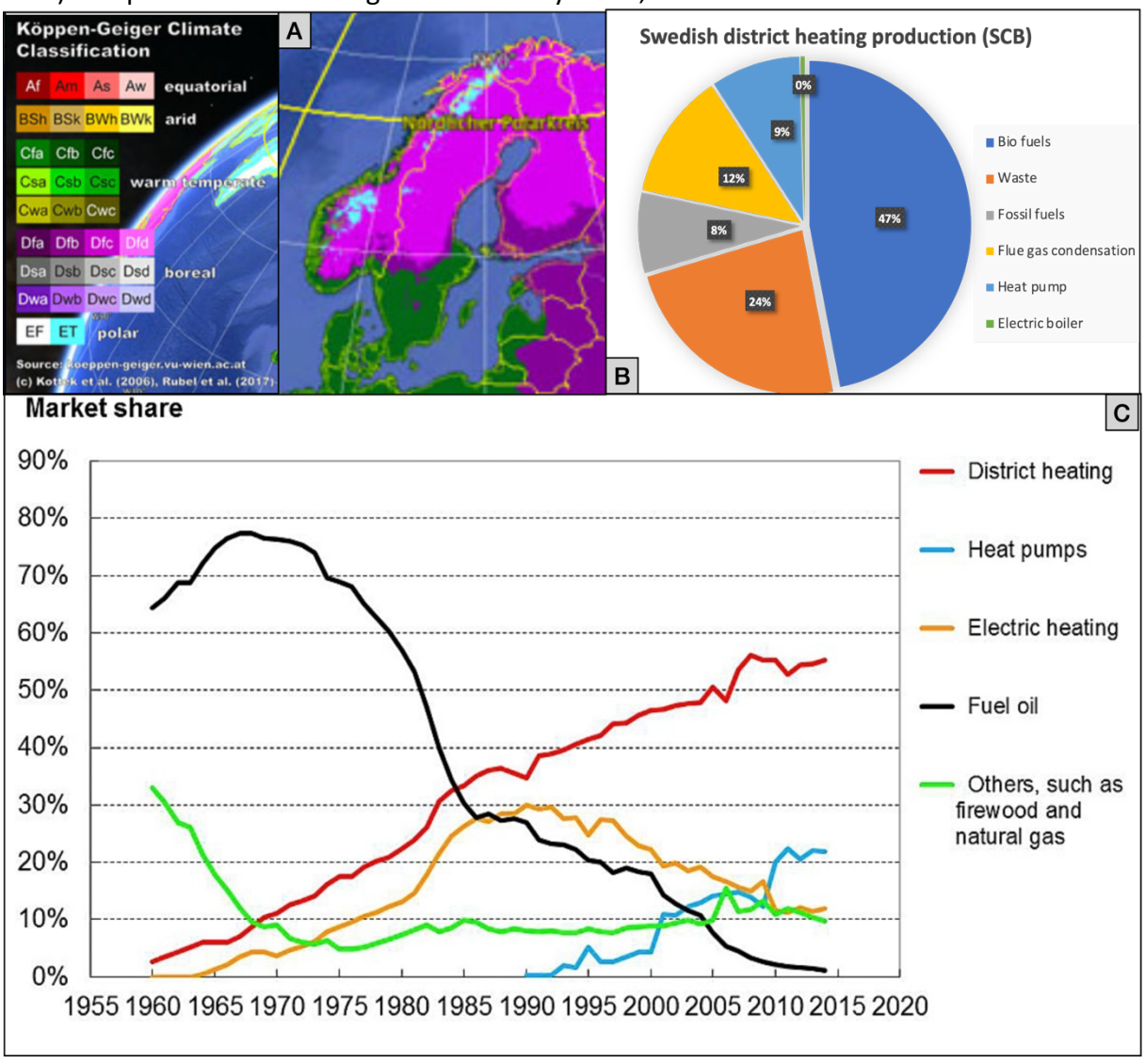

Figure 1. A) Köppen-Greiger Climate classification of Sweden (from koeppen-greiger.vu.ac.at). B) Average sources for district heating production in Sweden 2020 (from www.scb.se/hitta-statistik/statistik-efter-amne/energi/tillforsel-och-anvandning-av-energi/arlig-energistatistik-el-gas-och-fjarrvarme/pong/tabell-och-diagram/fjarrvarme-gwh/?menu=open). C) Market shares for heat supply to residential and service sector (from Werner, 2017).

particles causing air pollution. To avoid heat losses in the district heating system, the production plant is usually situated in the populated area it serves, hence the transportation associated with the production cause noise and more air pollution. The combustion from waste is the dirtiest from an environmental perspective. Despite that, and as more Swedish citizens recycle, more waste is being imported from foreign countries such as Great Britain and Italy (Naturvårdsverket, 2022), hence it can no longer be defined as a local fuel source.

What if there is a heat source without air pollution, emissions or heavy transportation? Everywhere on Earth, a perpetual heat source, exists: geothermal energy. Geothermal energy is usually extracted for electricity production or heating in places with naturally high geothermal gradients, rock permeability and water content. These areas are often associated with surface exposures such as hot springs, geysers and fumaroles, mostly found near plate boundaries (Figure 2). The exploitation of these **conventional** hydrothermal settings is increasing both for electricity and heating production (Figure 3A-D). However, most population centers are not located at such settings and are here referred to as **unconventional** hydrothermal settings. Since the 1970s, research has been carried out to artificially induce permeability at depth to utilize the heat in unconventional settings. These systems are usually called Enhanced Geothermal Systems (EGS). For any rock type at depth, lithostatic pressure causes a decrease in porosity which results in decreased permeability, permitting low or zero natural fluid flow. For crystalline rocks, almost all permeability is restricted to zones of brittle deformation (Tester, 2006). A variety of stimulation methods have been tried using hydro fracturing, hydro multi-fracking, hydro shearing, chemical and thermal stimulation, proppants and even explosive detonations (Parker, 1999; Pratiwi et al., 2018; Tester, 2006). The accumulated knowledge from these

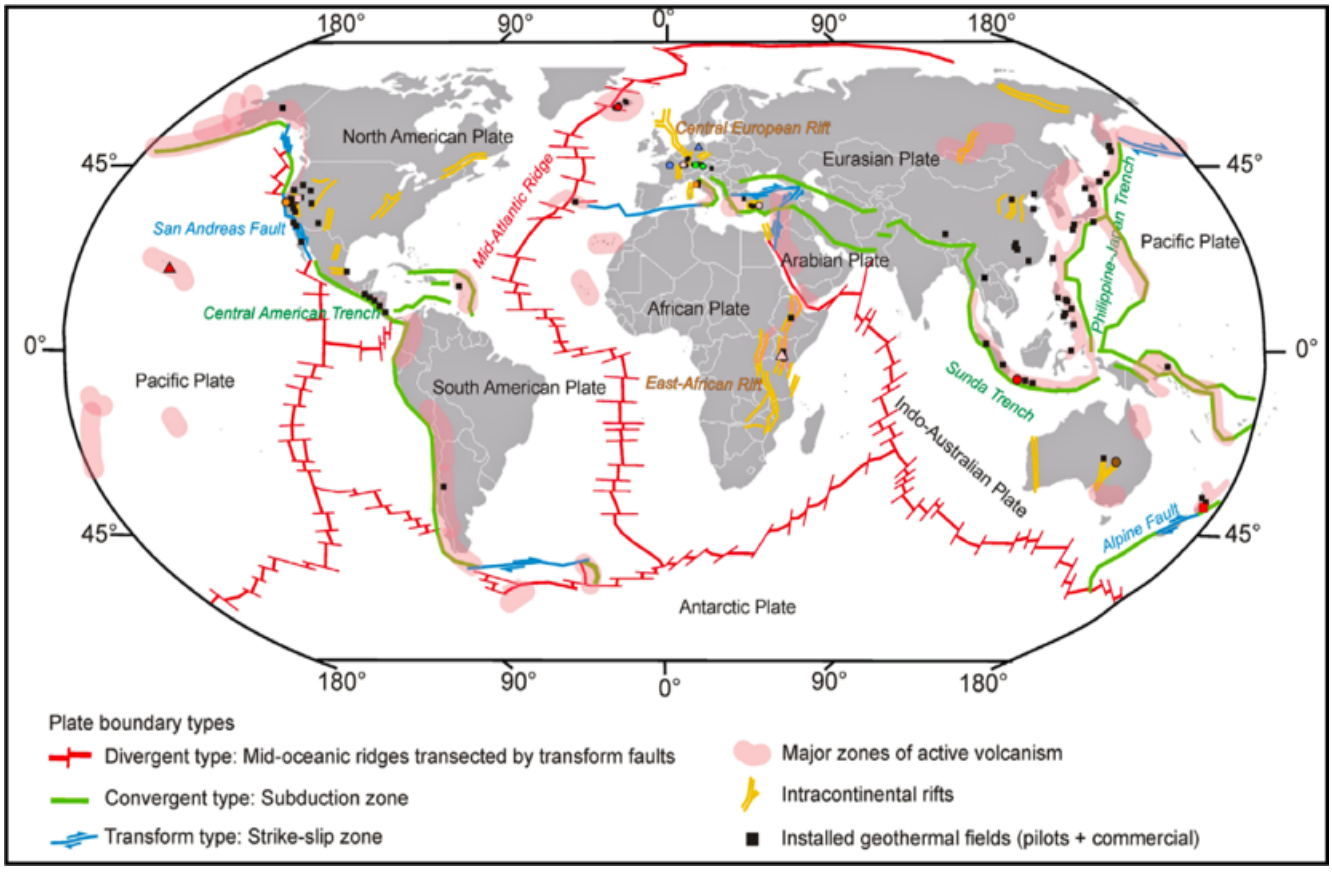

Figure 2. World map showing the distribution of different tectonic regimes and its correlation to commercial hydrothermal power plants (from Moeck et al., 2014).

developments shows that understanding the geological setting is key to efficient extraction of geothermal energy from depth. In this interview-supported literature review, the six deepest EGS projects in crystalline rocks have been evaluated, along with two unsuccessful attempts in Skåne with the goal to assess the chances of a future EGS success in Sweden. The result shows that there is a significant chance to extract deep geothermal energy even in the old, cold, and 'tectonically dead' Swedish part of the Fennoscandian Shield (FSS). The key might be in the geological interpretation made from the collected data for each EGS project and in delicate engineering.

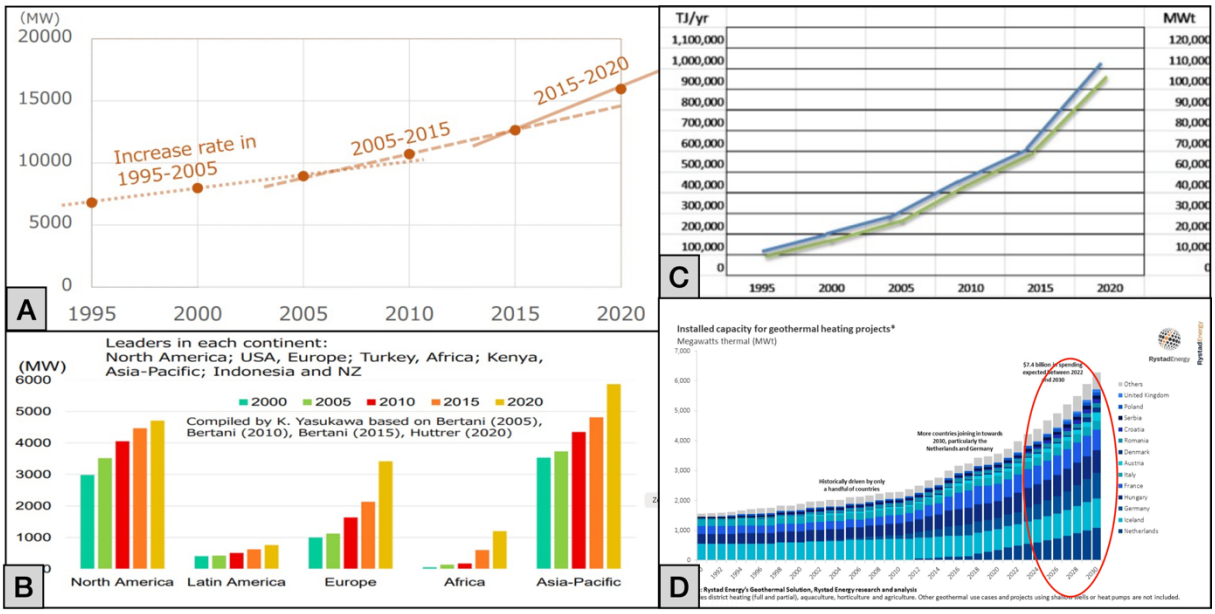

Figure 3. A) The increase in electrical geothermal power since 1995 (from Huttrer 2020). B) The increase in geothermal power for each continent (from Huttrer, 2020). C) The accumulated capacity for geothermal district heating systems (from Lund & Toth, 2021). D) Growth of capacity and estimated future capacity based on investments (from Rystad Energy 2022).

Background

History of geothermal energy use

The delivery of thermal energy from a central source is not a new idea. During Roman times, warm water was circulated through open trenches to provide heating for buildings and baths in Pompeii (Ozgener et al., 2007). Hundreds of years later, in Chaudes Aigues Cantal in France, geothermal water was distributed in the 14th Century through wooden pipes. That system is still being used (Ozgener et al., 2007). The first geothermal district heating system in the United States was created in Boise, Idaho, in 1892 (Tester, 2006). The second one was not constructed until 1964 in Oregon Institute of Technology (Tester, 2006). The 1980s saw a rapid increase in the number of geothermal district heating systems in the US and Europe, and the last decade it is again increasing rapidly (Figure 3C,D). As a response to global climate change, the uncertain supply of gas from Russia and a growing demand for new sustainable energy sources, an even steeper increase is predicted, especially for Europe (Figure 3D). Additionally, new generations of district heating systems, with lower temperatures aiming to reduce the heat loss is being developed for the future ((Werner, 2017)w).

Geothermal electricity production started in 1904 in Larderello, Italy, where geothermal water heated by an active magmatic system produced the first steam, driving

turbines for generation of electricity (Moeck, 2014). The geothermal power generation at Larderello proved to be commercially successful and is now one of the largest geothermal power plants in the world (Barbier & Fanelli, 1977; Moeck, 2014). But it wasn't until the oil crash in the 1970s that geothermal power research intensified, and this capacity has been growing steadily since (Figure 3A,B). In the same period, research for electricity producing EGS commenced the Fenton Hill, New Mexico (see Enhanced geothermal systems (EGS) below).

Basic principles behind geothermal energy

There are three main parameters controlling the conventional grade of a geothermal resource: (1) the geothermal gradient, (2) rock/reservoir permeability, and (3) water content. The inclination of the geothermal gradient controls the power of the heat source. The rock permeability controls the degree to which the rock can be used to exchange heat through the size of the reservoir and the fluid flow rate. (3) Due to its high heat capacity and abundance, water is a suitable fluid acting as an energy transport media. The natural abundance of water in impermeable rocks is, by definition, low. However, for an EGS, high natural abundance of water on the surface might be important for the development of a large reservoir (Tester, 2006). The geological settings that possess high values for each of the above parameters are usually restricted to tectonically active regions, i.e.- plate boundaries, where friction between the plates cause elevated geotherms and permeability through extensive faulting, volcanic activity and lithospheric thinning (Figure 2). Water is usually abundant in these areas since these boundaries are often constrained to oceanic environments with elevated or subsided topography (Tester, 2006).

From an economical perspective, geothermal heat is sold as energy (Watts), either through electricity (MW_{el}) or direct heat (MW_{th}). For electricity production, the hot water/steam drives a turbine that produces electricity, usually through secondary organic fluids with lower boiling points, driving the turbines in an Organic Rankine Cycle binary power plant (Tester, 2006). Thermal use has several applications: district heating, industrial purposes, agriculture, baths, etc. The customer, often an energy company, is interested in three basic outputs: Fluid temperatures (°C), fluid flow (l/s), and estimated lifetime of the system. The reservoir therefore requires a significant volume, so that the residence time of each water molecule has enough time to absorb the heat from the surrounding rocks (Jia et al., 2022; Tester, 2006).

Geothermal gradient

The geothermal gradient is expressed as the temperature increase with vertical depth. The heat source is suggested to emanate from (1) radioactive decay, (2) the primordial accretion of Earth, (3) release during differentiation as iron, nickel, copper descended to Earth's core, (4) latent heat released as the liquid outer core crystallizes at the inner core boundary, and (5) heat might also be/have been released due to tidal forces (Furlong & Chapman, 2013; Heller et al., 2021). According to the second law of thermodynamics, heat from the core is transported to the cooler surface. From the hot solid core, heat is transported through the liquid outer core by convection. The thermal mixing slows down in the more rigid and slowly convecting mantle where the heat is stuck at the Gutenberg discontinuity, which defines the lithosphere and asthenosphere boundary where temperatures are estimated to be c. 1350 °C (Rychert et al., 2020). From here, the heat it is transported through the lithosphere and to the surface via thermal conduction, where the heat reaching the surface is equivalent to the cooling of the Earth (Davies, 2010). The total surface heat flux, hence the cooling of the Earth, is estimated to 46 TW ± 2 (Davies & Rhodri Davies, 2010). Most of this heat is released from the oceanic lithosphere due to its thinner lithospheric thickness of 40-90 km, compared to the c. 130-200 km for continental lithosphere (Rychert et al., 2020). Heat flux measurements and bottom hole temperatures are determined by sensors placed in boreholes. To get the correct geothermal gradient, several paleoclimatological corrections need to be made due to the cooling from Pleistocene glacial periods (Kukkonen,

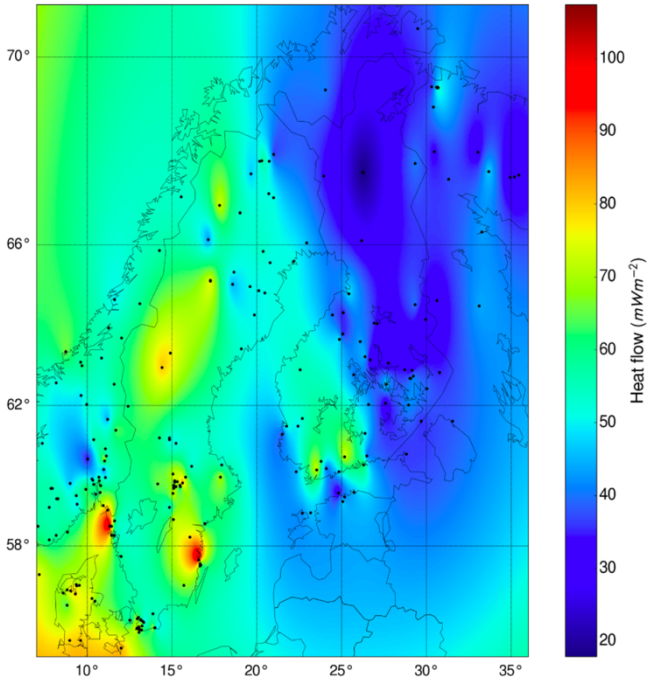

Figure 5. Paleoclimatically corrected heat flow map for Sweden, Finland and adjacent countries (from Veikkolainen et al. 2017)

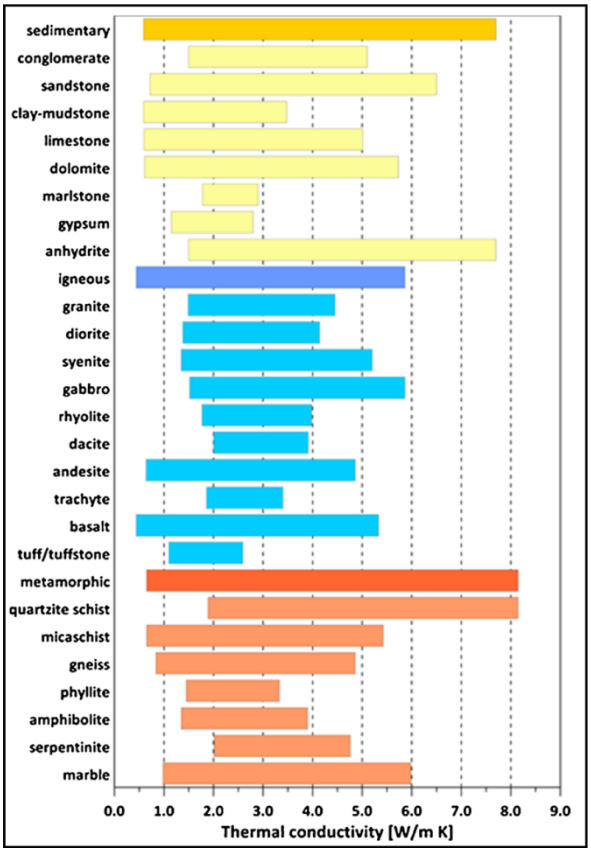

Figure 4. Thermal conductivity of different rock types based on porosity and pore fluid (from Della Santa, 2020)

1989; Slagstad et al., 2009; Veikkolainen et al., 2017). The most recent paleoclimatological corrected heat flow map of Sweden (Figure 5) is made by Veikkolainen et al. (2017). The relationship between heat flux and thermal conductivity is described by Fouriers Law:

$\Delta T = q/-k$ *Equation 1*

where q is heat flux (W/m^2), *k* is the material conductivity (W/mK) and ΔT is the geothermal gradient. Thermal conductivity can be measured in-situ through Thermal Response Tests or by laboratory measurements performed on specimens collected from each layer of the geological sequence under investigation. Typical values for various rock types are presented in Figure 4 (Dalla Santa et al., 2020). Even though Fouriers law is a one-dimension simplification assuming a homogenous lithosphere, it provides an understanding of the natural principles of the relationship between geothermal gradients and thermal conductivity. Using Fouriers law (Equation 1), a surface heat flux of 50 mW/m^2 and a thermal conductivity of 2.5 W/mK, which is typical for granite, gives a geothermal gradient of 20°C/km:

$\Delta T = q/-k \rightarrow 50/2.5 = 20$ *Equation 2*

However, due to the wide spread of thermal conductivity values (0.9 to 4.9 W/mK for gneiss), estimated geothermal gradients with a surface heat flux of 50 mW/m^2 may vary between 10 and 55 °C/km according to Fouriers law. Thermal conductivity is controlled by temperature, porosity, degree of saturation, pore fluid, dominant mineral phase, texture and anisotropy (Dalla Santa et al., 2020).

The geothermal gradient can vary drastically depending on the abundance of the heat producing radioactive elements Thorium (^{232}Th), Uranium (^{235}U) and Potassium (^{40}K). Granitic rocks have relatively high concentrations of U, Th, and K. However, this is the least known parameter because heat production does not correlate with other rock properties such as seismic velocity, density, etc. (Artemieva et al., 2017). Since radioactive decay decreases with time, heat production also decreases with age, but in a non-homogeneous way because the major radioactive isotopes in crustal rocks(U, Th, and K) have different concentrations and different decay constants (Artemieva et al., 2017). For example, the relative contribution of ^{232}Th to heat production decreases more slowly with time because this element has the longest half-life of the three isotopes, while the contribution of ^{235}U has a more rapid decay. Isotopic abundances are also highly variable. For example, radioactive ^{40}K makes only a tiny fraction of potassium isotopes, which are dominated by nonradioactive ^{39}K (ca. 93%) and ^{41}K (ca. 7%). On the whole, available data indicate that (except for low-radiogenic oceanic arc granites) post-Archean rocks have higher concentration of heat producing elements than Archean rocks (Artemieva et al., 2017). In order to calculate the heat flow from radioactive elements, Rybach (1988) suggested:

$$A\left(\mu \mathrm{Wm}^{-3}\right) = \rho(9.67C_{\mathrm{U}} + 2.56C_{\mathrm{Th}} + 2.89C_{\mathrm{K_2O}}) \times 10^{-5} \qquad \textit{Equation 3}$$

Where A is the heat produced, *p* is density, Thorium (Th) and Uranium (U) is in ppm and Potassium (K) in percent. Hence, the geothermal gradient is mainly controlled by lithospheric thickness, thermal conductivity, the abundance of heat producing radioactive elements, and volcanic activity. However, this is only based on the conductive transport of the heat. In

reality, fluids transport and distribute heat through permeable pathways in the lithosphere, which cause local heat flux anomalies. These permeable pathways are described below.

Permeability

The ability of a material to let a fluid through is called permeability (m^2). It is part of the proportionality constant in Darcys's law which relate to flow rate *v* (m/s) and fluid physical properties *n (*viscosity, *Pas*) to a pressure gradient ΔP (Pa) applied to the porous media (Equation 4). Its related to the more specific hydraulic conductivity (m/s), describing the material ability to allow water flow through it (Equation 5). Here, *k* is the permeability, *K* is hydraulic conductivity*, p* is the density of the fluid (kg/m^3) and *g* the gravitational acceleration (m/s^2). Since this study look at various fluids, like geothermal brines, the wider term permeability is used.

$$k = v\frac{\eta \Delta x}{\Delta P} \qquad \textit{Equation 4}$$

$$k = K\frac{\eta}{\rho g} \qquad \textit{Equation 5}$$

Permeability may come in the form of interconnected pore space, especially in sediments and sedimentary rocks, or as fractures in stronger rock types (Tester, 2006). In sedimentary rocks, there is a relatively regular permeability decrease due to compaction and diagenesis as depth and temperature increase. In basement rocks and deep sedimentary rocks, permeability is related to brittle deformation structures and the stress regime (Figure 6B)(Tester, 2006). Ingebritsen & Manning (1999) summarized a generalized distribution of crustal permeability with depth through geothermal data and estimates of regional metamorphic fluid flow (Figure 6A). Large-scale crustal fluid flow indicates a significant change over the permeability range of 10^{-17} to 10^{-13} m^2 down to c. 10 km (Ingebritsen & Manning, 1999). At the smaller value, the crust is basically impermeable; while, at the larger value, large-scale fluid flow is possible with significant reconfiguration of heat transfer and crustal temperatures (Wisian & Blackwell, 2004). This permeability, however, is not very useful for a geothermal reservoir, where fluid

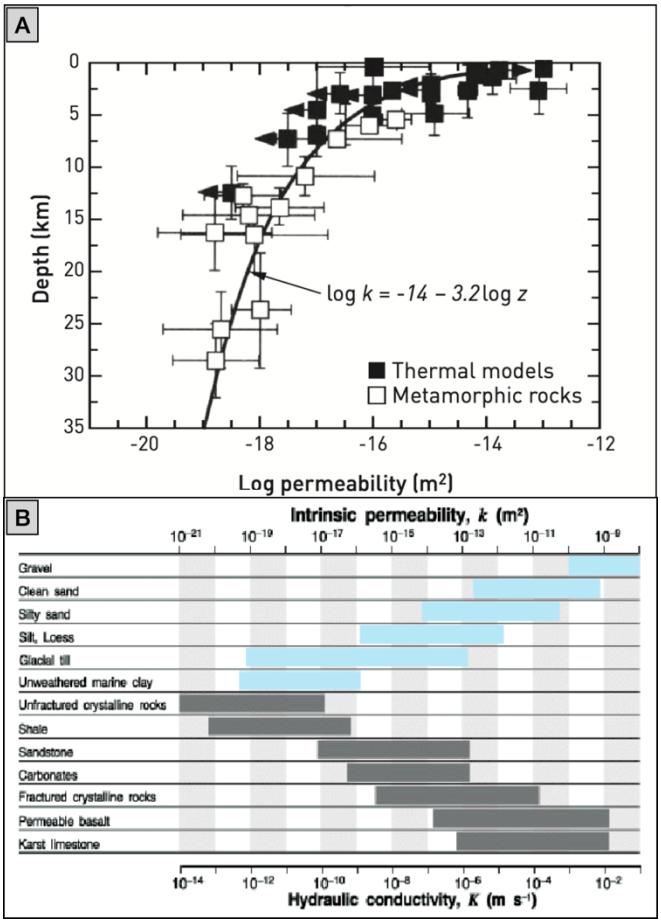

Figure 6. A) Permeability as a function of depth (from Ingebritsen and Manning, 1999). B) Showing the relationship between hydraulic conductivity and permeability and typical values for some geological materials (from Hornberger et al., 1988).

flow needs to be significantly higher. This permeability can only be found in open fractures. These fractures are naturally related to the deformation events that have affected the rocks. The openness of these zones are highly constrained by the current stress field. Ito & Zoback (2000) showed that permeable faults and fractures associated with thermal anomalies lie close to the Coulomb failure line, indicating that critically stressed faults at depth are the most permeable. Conversely, non-critical stressed fractures are not permeable (Ito & Zoback, 2000). From the Kola superdeep borehole, Kozlovsky (1984) described fluid-filled fractures at 9 km, although it is not well understood how such high-permeability fractures can persist under a confining stress of several hundreds of MPa (Ito & Zoback, 2000). Most deep fractures are permeable right after their formation, but over time hydrothermal conditions cause sealing and healing due to water/rock chemical reactions that significantly reduce the permeability. While shearing a fracture induces permeability due to brecciation and increases in porosity, but also due to the roughness of the fracture plane and breakdown of seals along the fracture plane (Ito & Zoback, 2000). As a result of the range of variation and the uncertain controls on the type and nature of permeability, it is generally thought that most deep, hot regions of the crust away from tectonic activity will require extensive characterization and subsequent engineering of a reservoir to be productive (Rosener & Géraud, 2007).

Geophysics

Coring and borehole imaging provide only local structural data. Extrapolation of these small-scale fractures at reservoir scale is problematic due to local differences and unpredictable fracture networks. Linking borehole data and surface data is also complex, but is necessary for understanding structural and hydraulic features of fractured media (Place et al., 2011). Surface geophysical techniques allow the investigation of the largest structures in a reservoir, but their restricted resolutions prevents efficacy at smaller scales (Place et al., 2011). Surface seismic reflection methods are not efficient for delineating dipping faults in crystalline basement due to the lack of subhorizontal reflectors and due to the acquisition and processing parameters which are not adapted to such targets. Therefore, combining vertical seismic profiles (VSP) with the surface seismic profile is recommended. Another way to use seismic data is described in the EGS section under *Microseismic modelling.*

Physical property / Target	Density	Magnetic susceptibiity	Electrical resistivity	Dielectric permittivity	Seismic velocity
Porosity	Strong	None	Strong	Moderate	Moderate
Permeability	None	None	Weak	Weak	Weak
Water content	Moderate	None	Strong	Strong	Moderate
Water quality	None	None	Strong	None	None
Clay content	Weak	None	Strong	Weak	Moderate
Magnetic mineral content	Moderate	Strong	Weak	None	None
Metallic mineral content	Strong	None	Strong	None	Moderate
Mechanical properties	Moderate	None	Moderate	Weak	Strong
Subsurface structure	Moderate	Moderate	Moderate	Strong	Strong

Strong | Moderate | Weak | None

Degree of relationship

Table 1. Summary of the relationship between geophysical methods and the specific target (from Manzella, 2016)

Other typical geophysical methods used to understand the subsurface include resistivity through magnetotellurics (MT), as well as gravity and magnetic susceptibility studies. Resistivity can show deep anomalies of higher porosity and water content at great depths. These zones can, however, also be alteration minerals with similar, or even lower, resistivity values than water (Manzella, 2016). Gravity can be used to interpret lithological

boundaries, such as the extent of a granitic batholiths to interpret radioactive heat production, but it also detects higher porosity and water due to their relatively low density. Magnetic susceptibility is related to the iron concentration in the rocks (hematite and magnetite). It can be used to detect low magnetic anomaly lineaments with oxidized shear zones (Henkel & Guzmán, 1977). A summary of the relationship between geophysical methods and the target is given in Table 1.

Enhanced geothermal systems (EGS)

In 2006, Massachusetts Institute of Technology released the book The Future of Geothermal Energy (here referred to as Tester, 2006). In this book, Tester highlights the immense potential of deep geothermal energy as a new renewable energy source for electricity production and heating all over the world. However, it would require further development of artificially induced geothermal reservoirs (EGS). They estimated that 10-15 more years of research and development was needed to make the technique viable. Now, 17 years later, several attempts have been carried out but no profitable EGS for crystalline rocks > 4 km has yet been developed. However, they seem to have contributed enough research and technological progress to keep the interest highly topical. In Sept 2022 the US announced an effort to reduce the cost of EGS by 90% via:

- Reducing the costs of drilling, well casing, and other materials and equipment.
- Development of advance engineering techniques to drill longer, wider wells faster.
- Collection of more and better-quality data to better understand the subsurface and more accurately predict the best locations for geothermal drilling.
- Ensure new reservoirs and all geothermal fluids contained to specific subsurface areas.

In China, EGS development was absent until about 2010, when several projects were initiated (Chang et al., 2020). According to China's long-term energy plan, geothermal energy will account for 3% of the energy consumption in year of 2030. This includes intensive R&D on EGS, aimed at both heating and power generation (Chinese Gov Announcement, 2021; Fang-chao et al., 2022). In 2011, the International Energy Agency (IEA) presented a roadmap stating that by 2050 more than half of the projected increase in geothermal power production would come from exploitation from EGS (IEA, 2011). In the EU, the DEEPEGS project was initiated in 2015 to demonstrate the feasibility of enhanced geothermal systems (EGS) for delivering energy from renewable resources in Europe (Fridleifsson et al., 2016).

Enhanced permeability

The main EGS concern has been how to artificially develop and control a sufficiently large reservoir with sufficient fluid flow rates between the injection well and the production well with reasonable added pressures (Tester, 2006). As described under *Permeability,* fluid flow in crystalline rocks is restricted to zones of brittle deformation. The fracture pore space forms interconnected networks of open space filled with an aqueous fluid. Deep geothermal energy development extracts this hot fluid via wells, removes the thermal energy and injects cold fluid to be reheated in a closed-loop system. Pumping tests in the boreholes provide hydraulic information and permeability data of the reservoir formation. The tests also supply samples of the pumped water for chemical analysis (Stober et al., 2022). Permeability increases can be achieved through various 'stimulation' methods such as hydraulic, chemical, and thermal stimulation. Among these, hydraulic stimulation is the most

commonly used technique to increase both reservoir permeability and the specific area for heat exchange (Jia et al., 2022). The stimulation techniques below can be executed with different strategies in time and space (Li et al., 2022).

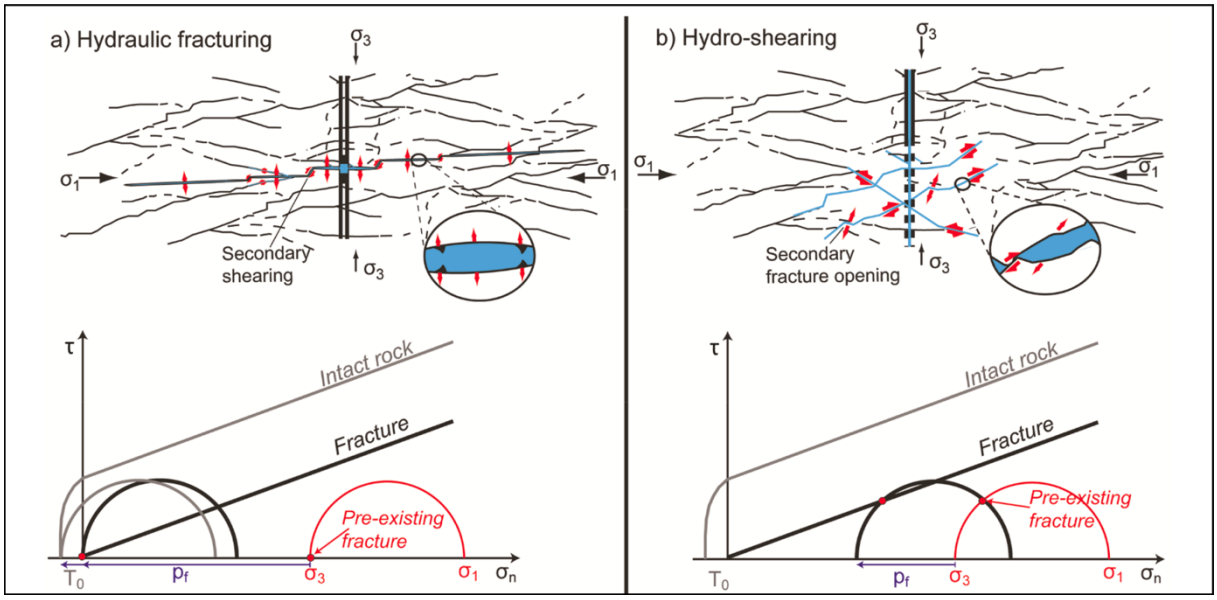

Figure 7 (a) Hydraulic fracturing opens new or pre-existing tensile fractures with fluid injected at a pressure higher than the minimum principal stress σ3. (b) Hydro-shearing aims to reactivate natural pre-existing fractures favorably oriented for shearing with a fluid pressure remaining lower than σ3 (From Gischig & Preisig, 2015)). The difference between HF and HS is also shown in a Mohr diagram below.

Hydro-fracturing and hydro-shearing

During hydro-fracturing (HF) new tensile fractures are propagated from the borehole when a fluid pressure is overcoming the minimal principle stress plus the tensile strength of intact rock (Figure 7a). Fluid injection is performed over small packed intervals in the open hole to create a stack of hydraulic fractures (Gischig & Preisig, 2015). During hydro-shearing (HS), over-pressure induces slip along pre-existing fractures that are favorably oriented in the stress field for reactivation in shear (Figure 7b) (Gischig & Preisig, 2015). HS stimulation is usually performed in a larger packed interval or in an open borehole. Which mechanism occurs predominantly during stimulation depends on the rock mass structure and in-situ stress field, but also on the orientation of discontinuities intersecting the open-hole section and thus being pressurized. Both mechanisms also differ in how they affect fracture permeability. While permeability gained by HS is mostly irreversible due to rearrangement of roughness contacts accompanied with shear dilation, permeability enhanced during HF reduces nearly proportionately after pressurization unless a proppant is used to ensure permanent apertures (Jia et al., 2022). Many observations and models indicate that HF may have a higher tendency of being aseismic, while seismic events associated with HS may be felt (Gischig & Preisig, 2015).

Chemical stimulation

Injection of fluids with chemical additives into the geothermal system can be used to reduce scale buildup in the borehole and dissolve secondary mineralization in the fracture network, leading to dissolution of certain minerals and thus increasing the fluid pathways in the rock to enhance the permeability. Chemical stimulation can be performed in acid soluble rock

formations such as carbonate rocks. Type and composition of the acid is determined by the mineralogy of the rock to dissolve the damaging material (Jia et al., 2022; Tester, 2006).

Thermal stimulation

When the working fluid is injected into hot reservoirs, it creates a traction force in the rock matrix that exceeds the rock tensile strength, and forms new fractures and/or secondary fractures. The stress reduction induced by thermal unloading is linearly dependent on the temperature difference between the injected fluids and the rock formation, as well as the bulk modulus of the rock. With the same temperature difference, brittle granite-based EGS reservoirs tend to be more sensitive to the thermal unloading effect (Li et al., 2022).

Induced seismicity

As the injected fluid cracks the reservoir rock, rock failure induces propagating waves, which are recorded as seismic events. From a reservoir performance perspective, these events are considered positive, indicating fracture fluid flow enhancement (Tester, 2006). However, large magnitude earthquakes are unwanted. If the magnitude of the triggered seismic event is above a certain criterion, usually M 2.0–3.0, the seismic event may damage surface structures, thus resulting in public safety concerns (Häring, 2004). The largest recorded magnitude of the earthquake related to EGS stimulations is up to ML 5.4 in Pohang and ML 4.6 in the Geysers in the US (Li et al., 2022). The precise mechanisms of the induced seismic event remain largely undetermined but the basic understanding of the implication of the stress regime, as simplified by Ulutaş et al. (2020) in Figure 8, is important to understand. Nonetheless, some key insights about the physical mechanism have been achieved:

- The magnitude of induced seismic events is highly dependent on injection volume (McGarr, 2023).
- A higher Young's modulus, e.g.- igneous rocks, in general corresponds to a larger earthquake magnitude. A lower matrix porosity implies that much smaller volume of injected fluid is required to trigger the same magnitude of earthquake. Therefore, igneous rocks could possess significantly higher risks of stimulation-induced earthquakes compared to sedimentary rocks (Li et al., 2022).
- The magnitude of triggered events is found to be dependent on the length of the pre-existing faults (Kwiatek et al., 2019)
- The temperature contrast between the injection fluid and the in-situ formation imparts significant effects on the magnitude and frequency of induced events (Li et al., 2022).

To mitigate triggering of high magnitude events, a traffic light system (TLS) can be used. The TLS involves careful monitoring of seismic events over the duration of the stimulation procedure and adjusting operation accordingly, such as decreasing injection flow rate, reducing fluid pressure, shutting-in, or flowing-back, when the seismic magnitude or the peak ground velocity reaches a specific threshold, or when other unexpected observations occur (Jia et al., 2022). However, a TLS system is reactive, hence a proactive approach would be preferable in order to have as much control as possible (*pers comm*. M. Ask). As suggested by the U.S. Department of Energy, to decrease the risk of triggering high magnitude seismic events, screening the target field by following certain criteria is vitally important and the location of the reservoir should be chosen appropriately (Tester, 2006). Field operations and numerical studies have observed that active/near-critical stressed faults

should be avoided. Moreover, the distance between the injection spot and nearby residential areas should also be taken into consideration (Li et al., 2022).

Microseismic modelling

In microseismic imaging, the microseismic device detects the acoustic emission resulting from local rock failure. The collected information is then interpreted, and used to estimate fracture length and orientation. It should be noted that microseismic tests cannot capture all microseismic events underground. For instance, microseismic tests are unable to record low-frequency, slow-propagating microseismicity (also known as aseismic events) induced by the opening of tensile fractures, as well as by thermally-induced traction. Microseismic event monitoring gives a 3D, time-resolved pictures of event location and magnitude from which the fractured rock volume is inferred, but a quantitative understanding of how the event map relates to the flow paths that define the extent of the underground heat exchanger is not established. More credible methods for mapping tensile fractures and shear fracture cluster geometry resulting from hydraulic stimulation are needed (Jia et al., 2022; Li et al., 2022).

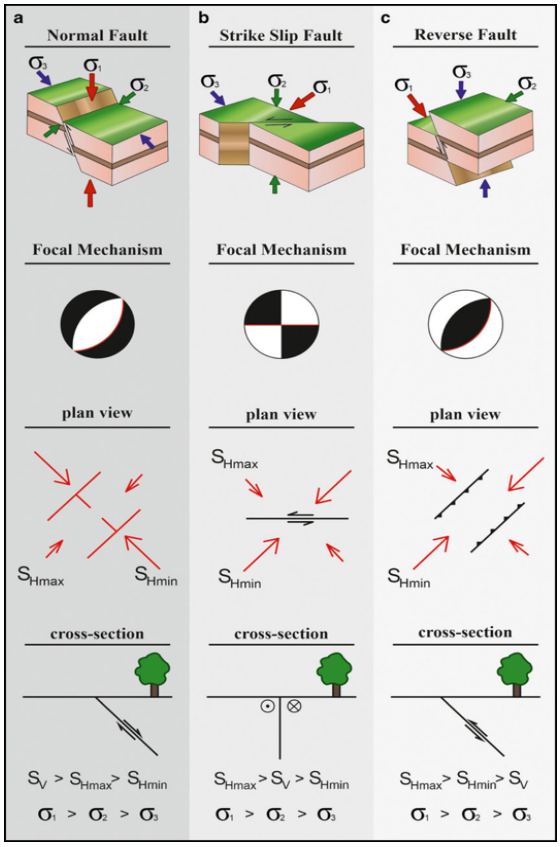

Figure 8. The basic principles behind tectonic regimes and how they are used to describe behaviour of brittle deformation (from Ulutas et al. 2020).

Advanced Geothermal Systems (AGS)

Instead of letting the fluid pass through permeable rocks, AGS is reducing the permeability issue by using advanced directional well systems. An AGS uses one or more wells drilled into hot rocks with fluid circulating through a closed-loop system to bring heat to the surface for direct heating and electricity applications. Several AGS designs have been proposed based on different geometries, heat transfer fluids, and physics principles. With current drilling technologies, AGS are economically non-viable (Malek et al., 2022).

Drilling techniques

The current drilling techniques used for deep wells are the conventional rotary or down the hole (DTH) percussion technique with rotation (Kervall, 2021; Tester, 2006; Todd, 1980). A large part of the deep EGS project investment is allocated to the drilling (Tester, 2006). Most deep (>4 km) wells today are developed for oil and gas exploration (Al-Darweesh et al., 2023). These wells are restricted to geological settings where oil and gas are present, i.e. in ancient sedimentary basins. They seldom need to drill in the crystalline basement, which limits the experience of drilling deep in crystalline conditions. Apart from the different lithology and the fact that at least two wells are needed, drilling deep geothermal wells is

more complex and expensive (cost/depth) than for oil, gas and mining exploration. Finger & Blankenship (2012) suggest these three reasons:

1. The technical challenge: the conditions high-T and high-permeability require special tools and techniques.
2. Large diameters: because the produced fluid is of intrinsically low value, large flow rates and thus, large holes and casing, are required.
3. Uniqueness: each geothermal well is more unique in the same field, than oil and gas wells in the same field, yielding more unexpected surprises during drilling.

Only rotary drilling can perform directional drilling and is therefore mandatory in the phase when/if the well is deviated to the target zone. The acoustics from the DTH can be used for making a VSP. Both techniques can use air, water, foam or mud as drilling fluid, with air and water is more common for DTH (Finger & Blankenship, 2012). The main parameters controlling the cost of a deep well drilling project is summarized in Table 2. These are mainly for rotary drilling, but can also occur with the DTH (from Finger & Blankenship, 2012).

	Additional costs	**Controls**
Small drilling hazards	Lost of circulation	- Managing fluid pressure
Large drilling hazards	Bottom hole assemblage stuck and drill string twists off	- Maintain borehole stability - Proper drilling fluid controlling swelling - Keep cuttings away from bottom when circulations stops
Rate of Penetration (ROP)	Extra time for renting the rig and service crew expenses	- Bit selection - Speed of rotation - Weight on bit (WOB) - Hydraulics/pressure control
Bit life	Tripping times and bit expenses	- Lithology - Drilling parameters (same as ROP, above) - Bottom hole assembly design
Directional drilling	Measure while drilling tools and directional motors	- Spatial knowledge of target
Well design	Cementing and casing	- Required flow rates and target depth

Table 2. The usual drilling parameters associated with significant additional drilling cost and how they are manually controlled, mainly for the rotary technique. Summary from Fingers and Blankenship (2012)

Planning and operating the drilling of deep wells require knowledge, experience and delicate fingertip skills (Table 2). First, it involves a drilling plan; one needs to decide the most suitable drilling technique, fluid and drill bit based on the rock types and structures that are expected at depth. It requires a conceptual model of the subsurface. However, a high-resolution model is never available for un-drilled locations, so the driller engineers needs to be utterly responsive during the drilling process. A constant and suitable weight on bit and fluid pressure must be supervised for an optimized rate of penetration (ROP). For deep wells, the 'holdback' force must be relatively high due to the total weight of the drill string acting on the bit (*pers comm*. L. Aman). With rotary techniques, cuttings become relatively small and since drilling is usually carried out with lubrication mud, the bottom

pressure becomes high enough to carry cuttings to the surface. The rotary technique has an average ROP of 1.5 m/h in crystalline rocks (Erlström, 2016).

For DTH, pressurized air and/or water usually bring the cuttings to the surface. DTH with air has the highest ROP in dry crystalline rocks, up to 30 m/h, but becomes not applicable in zones with high water inflow (*pers comm*. J.Rosberg). It is not possible to drill deeper than to the depth where the pressure of the water column approaches the available pressure in the drilling process. This available pressure also controls from which depth it is possible to bring the cuttings to the surface. In crystalline rocks, cuttings usually become larger than for sedimentary rocks, which require even more additional pressure to transport it to the surface. Therefore, water, air, and/or foam can carry cuttings up (*pers comm.* L Aman*)*. The reach for high ROP is pointless if the bit/tool life is low, hence the total time of a drilling project is in the end the most important (*pers comm.* J. Rosberg). It is therefore important to increase drill bit longevity and reduce the drill bit consumption for all drilling projects and, especially, for deep EGS drillings as a step to reduce the total cost. The time to replace a drill bit, e.g.- at 3 km depth, can take around 18 h and the daily drilling cost can be 30,000 Euros or higher (Energimyndigheten, 2021).

In the public debate, discussions are intense about promising drilling techniques. The US government funded company Quaise Energy, in collaboration with MIT, announce they are developing an entirely new technique including microwaves that vaporize the borehole (*Quaise Energy*, 2023). High power laser has been tried several decades and hasn't yet been successful, but current research is looking far more promising (*pers comm.* K. Mallin). Furthermore, the EU is now funding OptiDrill, an AI machine learning technique where drilling data are compiled in a database to develop an optimized drilling performance sensor system for different geological settings (*pers comm.* K. Mallin). In China, government owned LandOcean Ltd is now drilling an exploration and scientific well aiming to reach 9500 m, where Chinese National Petroleum Corp. (CNPC) announced that new innovations in drilling technologies shorten drilling time significantly (Zheng, 2023).

Geothermal energy in Sweden

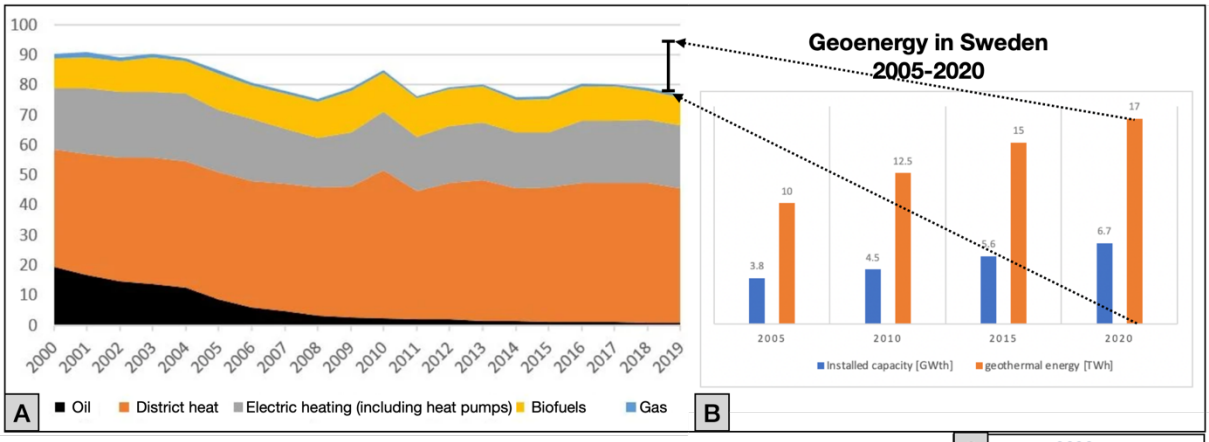

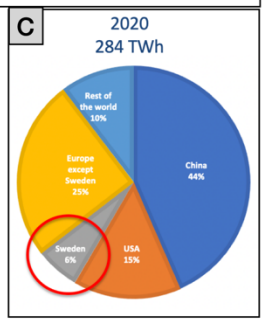

Figure 9. A) Showing the energy use for heating and hot water in small houses, large houses and offices (from Energimyndigheten, 2022), incorporated with the contribution of shallow geothermal energy use in Sweden, as presented in B (from Svenskt Geoenergicentrum, 2023). C) Plot showing the total geothermal direct energy use share for the world, where Sweden stands for 6 % (from Svenskt Geoenergicentrum, 2023, based on figures from WGC 2021; Lund et al, 2021).

Geothermal energy in Sweden is dominated by low temperature, shallow geothermal energy systems, and >95 % of installed geothermal energy systems are ground source heat pump systems for heating and hot water for single-family buildings (Gehlin et al., 2020). In 2020, shallow geothermal energy systems provided approximately 17.1 TWh of heating from the ground (no heat pump electricity included), with a half million installations (Figure 9B) (Gehlin et al., 2020). About 5 TWh of the electricity (to run the heat pump compressors) was needed to provide this heat. This means that an additional 17.1 TWh of heating, from the ground (Figure9B), should be added to the diagram in Figure 9A, thus increasing the total energy with 22%. This energy efficient heating method is one significant reason for the drop in electric heating starting in the 90s, as can be seen in Figure 1C. The installed heating capacity is 6 680 MW, which is a significantly high proportion of the global share of geothermal direct use (Figure 9C) (Gehlin et al., 2020). Over the last decade there has been an increase for larger shallow geothermal energy systems and boreholes are being deeper (Figure 10). There are today two high-temperature borehole thermal energy storages (HT-BTES) in operation in Sweden, one residential and one industrial application and more large-scale high-temperature storages connected to district heating plants are under consideration or investigation (Gehlin et al., 2020). Since 1984, there is a low-temperature geothermal heat production plant in operation in Lund, Skåne, providing heat pump supported geothermal heat to the district-heating network. It is still serving the district heating network with initially 25 °C water from a 750 m sandstone aquifer (Rosberg & Erlström, 2019).

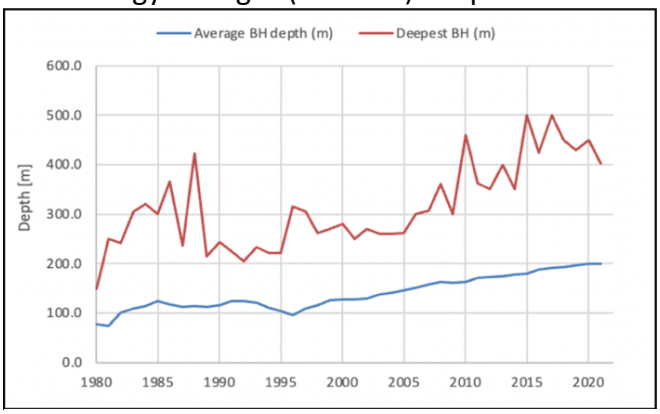

Figure 10. Borehole depth statistics showing the deepest and average borehole for shallow geothermal energy (from Svenskt Geoenergicentrum, 2023).

Investigation for deep geothermal exploration in Sweden

Initiated by the energy crisis in the 1970s, deep geothermal energy potential has been, and is being, explored in Sweden. The deep exploration projects carried out in Sweden are summarized in Table 3 and located on the geological map of Sweden (Figure 11). The Lund (2001) and Malmö (2017-2021) initiatives are part of the detailed case studies (see page 37).

Place/year	Developer	Result	Reference
Lund 1970-1984	Nämnden för energiforskning Lund University	2270 m (Höllviksnäs-1) testhole (30°C/km estimating 90 m³/h) Heat pump supported geothermal power plant in Lund, 20-25 °C sandstone aquifer at 400-800m	Andersson, 1980
Fjällbacka 1984-1995	Chalmers	Successful stimulation at 500m Connected wells through hydraulic shearing in fractured granite	Wallroth et al., 1999
Stockholm/Birka 1997-2004	Energimyndigheten KTH	Two 1 km testholes New stress/structural/geophysical data No permeability encountered	Henkel, 2007
Malmö/ Copenhagen 1995	SGU/GEUS Sydkraft (now E.ON) DONG (Danish oil corp) HGS (Danish geothermal corp)	Successful doublet of 20 MWth in Copenhagen at 2600 m. Now abandoned due to lead scaling	Energimyndigheten , 2021
Lund 1999-2001	Lunds Energi (now Kraftringen)	A 3701 m well was drilled Useful information from borehole	Rosberg & Erlström, 2019
Malmö 2002-2004 2017-2021	Energimyndigheten Sydkraft (Now E.ON.)	Two 2100 m wells into sandstone Tested a possible output of 10 MWth Cancelled due to “economical reasons” Part 2 cancelled due to high drilling cost	Rosberg & Erlström, 2021 Energimyndigheten , 2021 Juhlin et al., 2022
Göteborg 2021-2022	Energimyndigheten Göteborgs Energi	Less heat from Bohusgranite than hoped Fractures relate to linear valleys at surface, mafic intrusives and foliation planes Est. 120° at 7km which was to risky	Hogmalm et al., 2021

Table 3. Deep geothermal exploration projects carried out in Sweden.

Summary of Swedish geology

Lithology and ages

With regard to assumed differences in thermal properties, Swedish geology can be divided into three simplistic categories (Figure 11) (Hoseini, 2007):

- Pre-Cambrian Fennoscandian Shield (FSS)
- The Caledonides
- Phanerozoic sedimentary rocks

The Caledonides and the Phanerozoic sedim entary rocks sit on top of the FSS with varying thickness (Lorenz et al., 2015; Rosberg & Erlström, 2021). The core of the Fennoscandian Shield is located in the central parts of Sweden and Finland and chronologically extends from the NE older parts in Russia to the youngest parts in SW Norway (Figure 11). The FSS can be divided into sub-provinces based on its age (Figure 11). In Sweden, the FSS is basically made up by the magmatic Archenan Province (2.5-3.1 Ga) in NE, followed by the extensive Proterizoic subduction and back-arc related volcanism and magmatism during the NNE trending Svecofennian Orogeny (1.75-1.9 Ga) (Lundqvist, 2011). The end of the orogeny is associated with granite intrusions and deformation causing extensive shear zones. During Transscandinavian Igneous Belt (1650-1800), the direction of the subduction changed to the E and caused large felsic batholiths and volcanics, but also mafic and ultramafic intrusives (Lundqvist, 2011). Further SW, accretion continued to about 1.5 Ga, with some following anorogenic intrusions, ending with the Sveconorwegian Orogeny at 1-0.9 Ga (Lundqvist, 2011). The next 500 Ma includes spreading, sedimentation, collision, erosion, tectonic uplift

and more erosion on the western edge of the FSS. The result is the Caledonides, comprising accretions of mainly meta-sedimentary nappes (Lundqvist, 2011). The sedimentary rocks comprises a succession from Phanerozoic (55-545 Ma) limestone, sandstone and shale (Lundqvist, 2011). During the Quaternary period, ice sheets removed the top layers, leaving behind a significant amount of denuded bedrock.

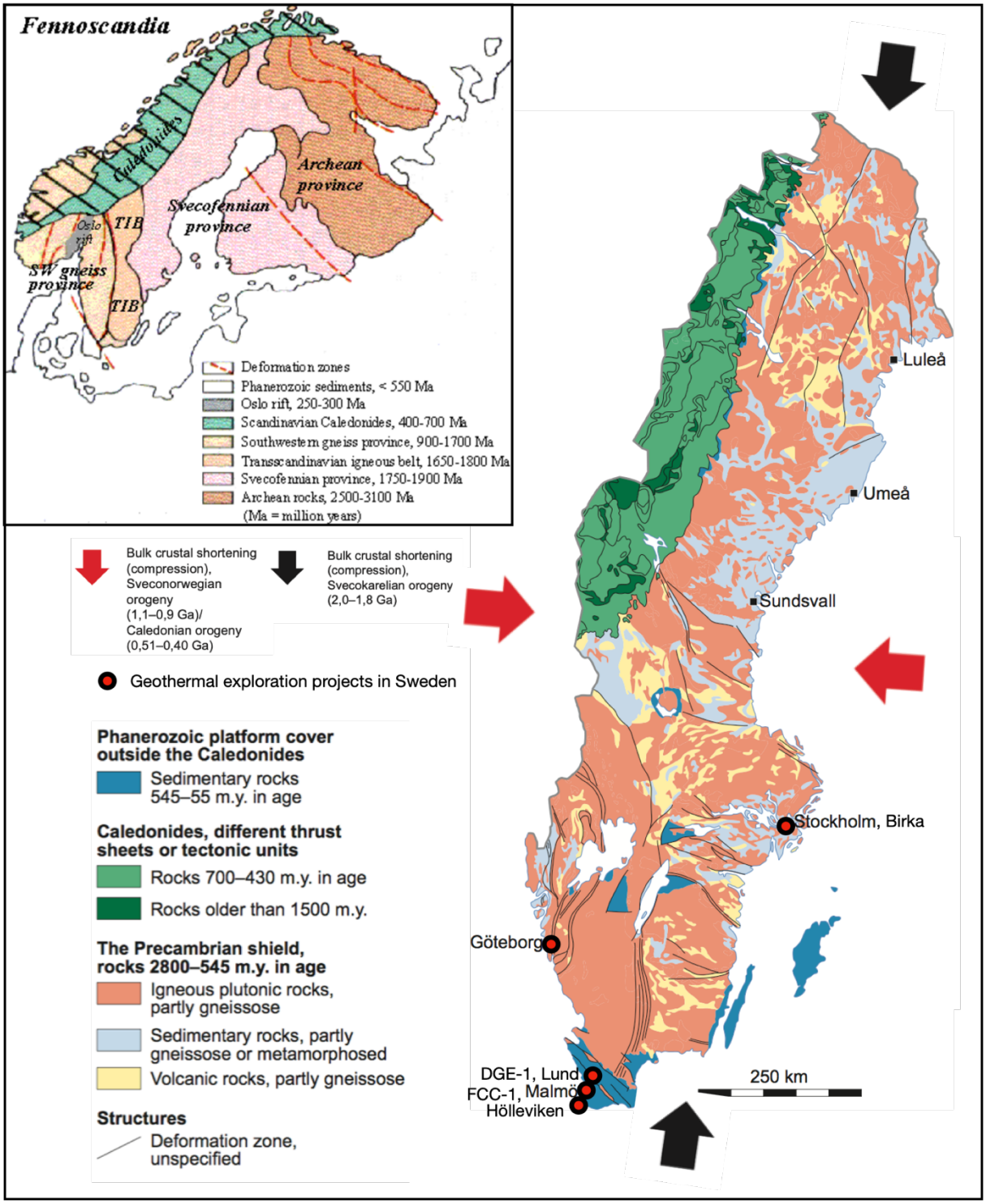

Figure 11. Inset shows the provinces in the Fennoscandian Shield (from Naturhistoriska Riksmuseet website: www.nrm.se/faktaomnaturenochrymden/geologi/sverigesgeologi/fennoskandiasberggrund). The simplified geological map of Sweden (from https://swedenunderground.com/how/geological-conditions/) showing the lithologies with ages and deformation zones. SHmax defined from the Svecofennian Orogeny event (back arrows) and Sveconorweigian/Caledonide Orogenies (red arrows). As red dots, the geothermal exploration projects summarized in Table 3.

Deformation

In a simplified overview of deformation, during Svecofennian orogeny, intensive shearing occurred in a N-S thickening regime (Lundqvist, 2011). In Sveconorwegian and Caledonides, E-W compression caused deformation and reactivation of shear zones and fractures (Baltybaev, 2013). Such structures are revealed by several km long linear structures on topographic, geophysical, and geological maps. The Sorgenfrei-Tornqvist zone is the only recent tectonic fault zone in Sweden, acting as a boundary between the old FSS to the NE and the younger geological provinces to the SW (Rosberg & Erlström, 2021). Furthermore, meteorite impact craters cause intensive fractures as can be seen from geophysical maps, and isostatic rebound from the Weichselian glacial period are now causing subvertical faulting in the north of Sweden, for example the Pärvie fault (Lundqvist, 2011).

Stress data

The current regional stress field in the Fennoscandian Shield is primarily caused by a horizontal tectonic pressure from the spread in the Mid-Atlantic Ridge. Ignoring local variations, the largest horizontal stress (σ_1) is generally orientated in a northwest–southeast direction in the southern half of Sweden (Wahlgren et al., 2019). In addition to the pressure of the Mid-Atlantic Ridge, postglacial isostatic rebound, cause a stress relief representing a second-order stress source (Uski et al., 2003). However, local differences occur as can be seen in the stress map of Heidbach et al. (2018) (Figure 12A). The significance of the rebound from the ice retreat on SHmax is debated, where Stephansson (1988) argue for a minimal effect on the stress, whereas Wahlström (1993) argue for a . Steffen et al. (2021) compiled a model a of stress from glacial retreat with associated early earthquakes in Figure 12B.

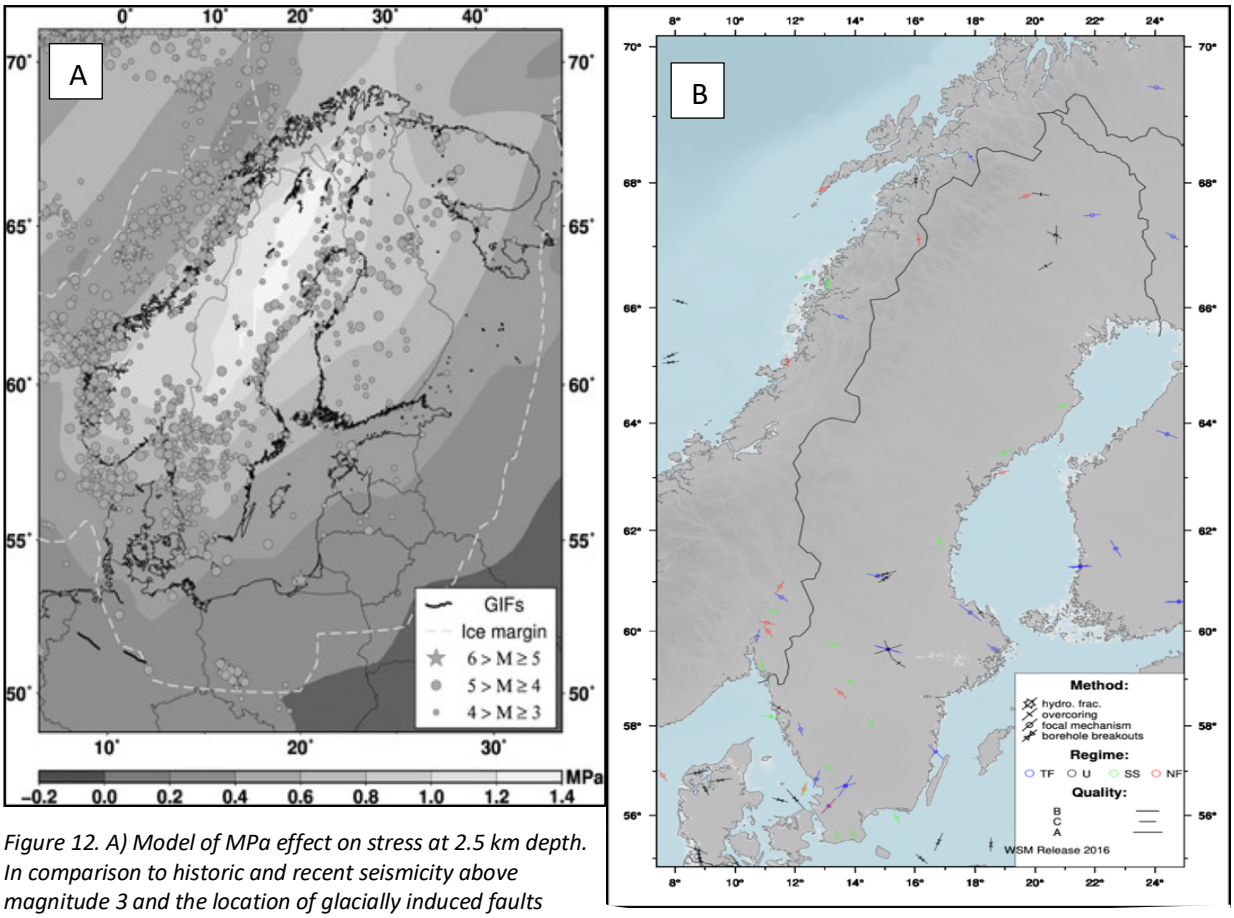

Figure 12. A) Model of MPa effect on stress at 2.5 km depth. In comparison to historic and recent seismicity above magnitude 3 and the location of glacially induced faults . Light grey dashed line is Last Glacial Maximum (from Steffen et al., 2021. B) Stress map from different sources giving an impression of the variety and local distribution of tectonic regimes and the orientation of SHmax in Sweden. The map shows the sparsity of in-situ measurements in Sweden (from Heidbach et al., 2018).

Methods

Literature review

The literature review involved in this study involved academic published reports, mainly obtained through the Stockholm University online library. In many cases, when reports weren't available, they were ordered as a paper copy and picked up at the Stockholm University library desk. A comprehensive amount of data, and suggested published reports of the basic principles and the lessons learned from the early EGS projects carried out between 1970-2005, comes from the book "The Future of Geothermal Energy, 2006", written by researchers from the MIT (Tester, 2006). Some information was gathered from governmental and corporate reports and from geothermal congress presentations and abstracts. In rare cases, newspaper articles were used. For the Habanero EGS project, much data was gathered from the comprehensively synthesized, 184 page corporate report "Habanero Geothermal Project Field Development Plan, 2014" (Humphreys, 2014) released by the project owner Geodynamics Limited when the project was terminated. The most challenging data to collect was from the ST1 and United Downs projects, since they are the newest ones and much information are not yet public due to confidentiality issues.

Interviews

In order to find suitable experts to interviews, two main strategies were used; (1) Personal contact, and (2) by contacting researchers and companies online. For the first strategy, the author basically used his personal network to find appropriate experts to interview. It was usually preformed via an initial email-contact with a description of the project and an explanation of how the interviews were to be executed. The person that recommended the expert was usually copied (cc) at first contact. If the expert accepted to be a respondent, s/he was sent an individual agenda and a Letter of Intent (A1). In the Letter of Intent, the following was explained for the respondent:

- The goals of the thesis and background information
- The interview motives
- The confidentiality and management of oral recording

Interviews were executed with the software Zoom (Zoom Video Communications, Inc., version 5.13.11) or email conversations. If data, statements, or opinions from the interviews were used in the report, it is referred to as personal communication *(pers comm.,* respondent*).* The oral interviews were transcribed and exported as .csv files with the software MacWhisper (version 2.17). The transcript was cleaned manually (see the example of cleaned transcript in Appendices (A2). The recordings and the transcripts were backed up in a hard drive for safety reasons and the computer was locked with a password.

Results

Eight EGS projects

The data from each EGS project from around the world (Figure 13) based on public literature and interviews are summarized here. The layout for each project is organized with text and figures as follows:

1. Background
    a. Project owner, intended reservoir target, output goals ($MW_{el/th}$), motivation of location and its drilling history.
2. The geology of the reservoir
    a. Lithology and ages, in-situ stress field, tectonic regime, deformation structures and geothermal gradient.
3. The result
    a. Operational strategy, drilling and stimulation result and main lessons learned.

Figure 13. World map with the studied EGS projects.

Soultz-sous-Forêts, France (1987-present)

Background

The European deep geothermal project was designed to exploit the potential energy of deeply fractured rocks for electricity production. This research project was initially funded by the European Community, Great Britain and German ministries and French ministry of research via the Energy and Environmental Agency, the Geological Survey and the National Scientific Research Center (Dezayes, 2005). Soultz was targeted instead of Cornwall, UK, because the predicted linear geothermal gradient with a temperature of >200°C at 2000 m, made it more feasible for electricity generation (*pers comm.* Y. Geraud). Based on oil exploration, an intense thermal anomaly was identified in this area. In some boreholes, geothermal gradients >110°C/km are recorded (Dezayes, 2005). This temperature anomaly matured the organic matter resulting in the famous Pechelbronn oil field (Durst, 2013; Place et al., 2018).

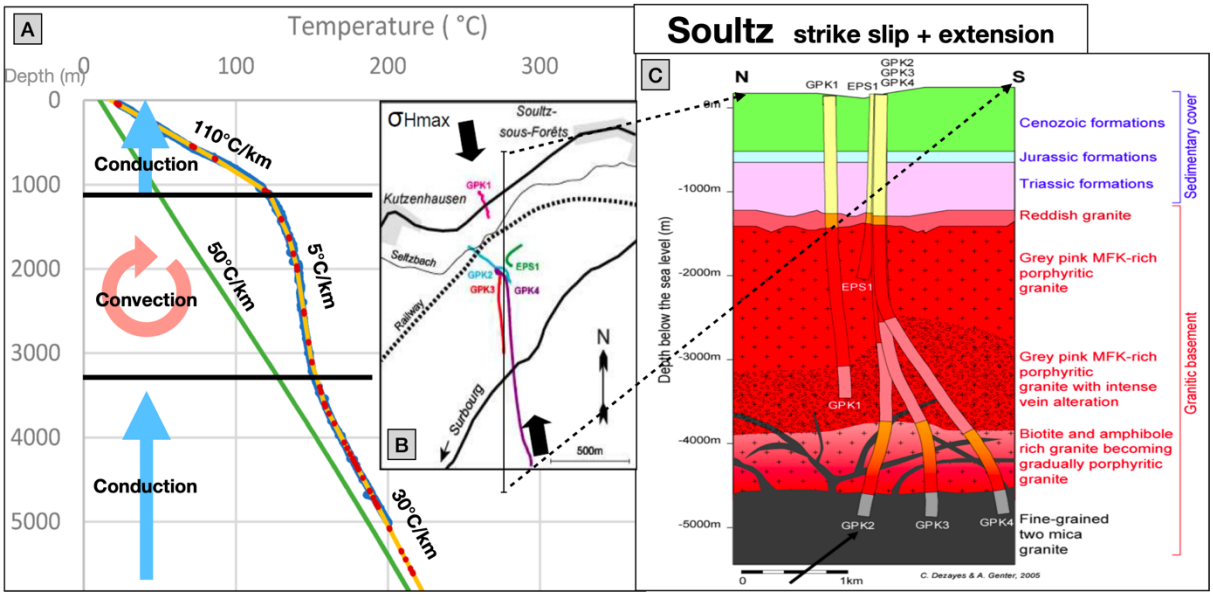

Figure 14. Soultz, France. A) The characteristic geothermal gradient from Soultz showing the conductive heat transfer in the sedimentary cap, followed by convection in the upper c. 2 km of granitic basement (modified from Durst, 2013). B) Map showing the SHmax orientation and the orientation of the wells (from Durst 2013) with the inferred cross section from C) Showing the stratigraphy and the orientation of the wells (from Dezayes, 2005).

The geology

The first 1.2 km is composed by Cenozoic and Mesozoic sedimentary rocks. This is underlain by Paleozoic granite basement developed during the Varascian orogeny (300-400 Ma) (4C). The tectonic regime is of oblique strike slip extension. SHmax is striking 82° (Figure 14B). The upper granitic basement at 1.2-3.5 km is severely fractured from Tertiary extension with a paleo-weathered surface, resulting in increased porosity (Bertrand et al., 2021; Dezayes, 2005; Durst, 2013). As a result, a convection cell of natural brine is mixing the heat in the fractured granite with the sedimentary cap above enclosing the heat. This cause a drastic decrease of the geotherm in the convecting zone (Figure 14A). Below this convection cell at ≥3500 m, the geothermal gradient is equivalent to the average geothermal gradient in Central Europe of about 30°C/km (Kölbel & Genter, 2017). In the lower basement, Tertiary reactivation of old brittle fracture zones and joint sets from the Variscan orogeny allows a workable volume of fluids, despite their deviating orientation with respect to the prevailing SHmax (*pers comm.* Y. Geraud).

The result

The project crew did not anticipate a geothermal gradient of about 5°C/km between 1.2 to 3.5 km. As a consequence, instead of reaching 200°C at 2000 m, they needed to go as deep as 5000 m. The work in Soultz has resulted in about 35 years of research, first from an upper reservoir in the convection cell at 2800-3600 m, and then from a lower reservoir in the conductive basement at 4500 - 5000 m:

Upper reservoir (drilled during 1991-1998):

A maximum stimulated pressure of about 14.5 MPa and a maximum flow of 50 l/s enhanced the permeability. The distance between the doublet (outflow and uptake) was 450 m. The output was 10 MW_{th}, with a production temperature of 140°C, without fluid loss. Acoustic monitoring showed the reservoir growing in a NNW-SSE direction, with a tendency for the fracture cloud to grow upward. One major and two secondary fracture sets formed a stimulated volume of about 240,000,000 m^3.

Lower reservoir (drilled during 1999-2007):

In 1997, private investors aimed to reach bottom hole temperatures of at least 200°C for electricity production. GPK-2 was deepened to 5000 m and two new wells were drilled to 5093 m and 5105 m making it a triplet well system with well bottom distances of 600 and 650 m spacing (Figure 14C). Hydraulic, thermal and chemical stimulations was performed to increase the permeability and the connectivity between the reservoir and the wells. As in the upper reservoir, their trajectories are distributed in the north–south direction; GPK-2 is the production well and GPK-3 and GPK-4 are used as injection wells. GPK-2 and GPK-3 have good connectivity, whilst GPK-4 does not. It is suggested that GPK-4 is separated by an aseismic zone (Baisch et al., 2010). In January 2011, a 1.5 MW_{el} power plant was successfully installed and provides power to the grid using a fluid flow of 19 l/s, production pressures of 18,5 bar and a production temperature of 160°C (Durst, 2013). This is a milestone enabling further research and investigations to meet new challenges resulting from operation, e.g.- scaling and corrosion, high temperature pump applications, induced micro seismicity monitoring, and enhanced coupled thermal–hydraulic–mechanical–chemical models for better reservoir understanding (Kölbel & Genter, 2017). In 2015-2016, the power plant renovated the ORC unit and now produces 1.7 MWe and about 11 MWth from a geothermal fluid at 150°C which is fully reinjected in the granite reservoir at 70°C with a fluid flow of 30 l/s (Baujard et al., 2018, 2021).

Basel, Switzerland – (2001-2008)

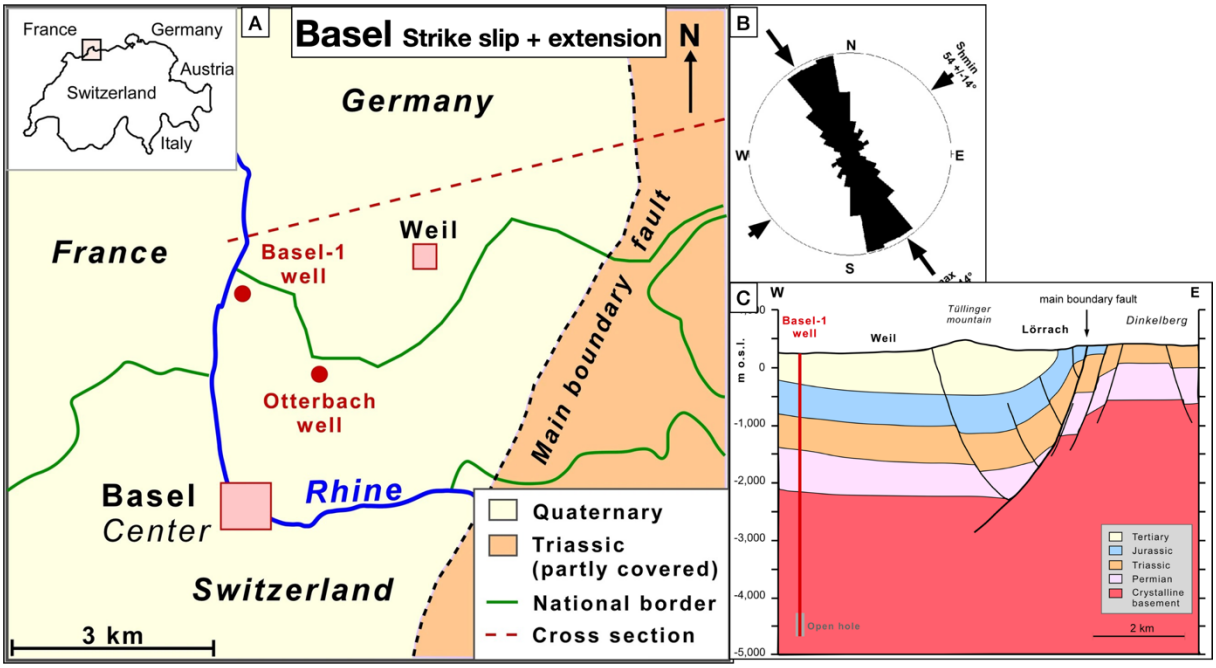

Figure 15. Basel, Switzerland. A) Location of the Otterbach 2755 m testwell and the 5000 m Basel-1 well and the main boundary fault (from Stober, 2022). B) Orientation of SHmax (Häring, 2008). C) Schematic cross section (see A) showing fractures in the sedimentary rocks and the main boundary fault pointing towards the open hole in Balse-1 (from Stober (2022).

Background

The Kanton of Basel-Stadt in partnership with a number of Swiss utility companies aimed to develop a geothermal 6 MW_{el} and 17 MW_{th} pilot power plant through an EGS (Swiss Seismological Service, 2017). The plan was to exploit the estimated temperatures of 200°C in the basement granites at about 5000 m (Häring, 2004). The Deep Heat Mining Project was developed and operated by Geothermal Explorers Ltd (Häring, 2008) and was due to be built in the city of Basel, i.e.- the first EGS project in an urban area (Tester, 2006). In 1356, the strongest earthquake in NW Europe destroyed the city of Basel (Meyer et al., 2007). Therefore, it was important to record and understand the natural seismic activity prior to stimulation of a deep reservoir. The exploration well, Otterbach-2, was therefore drilled in 2001 into the granitic basement at 2650 meters for a total depth of 2755 meters. This was the first well to penetrate the granitic basement in the area (Häring, 2004). The original concept was to generate a network of efficiently hydraulically interlinked, densely distributed fractures over a large rock volume with one massive hydraulic injection. It was intended to produce fractures associated with the main boundary fault system (Figure 15A,C). When the main target of 190°C and a fractured reservoir rock in a favorable stress field were found, the drilling would be suspended (Häring, 2004). A second monitoring well at 2 km to the east would then be drilled and equipped with a seismic array similar to the Otterbach-2 well. The two extended seismic arrays were to provide a series of locally independent receiver points, sufficient to compute the location of a seismic source with the required accuracy. Subsequently, injection tests will be conducted in the deep well in order to develop an EGS reservoir (Häring, 2004).

Geology

The granitic basement is overlain by Quaternary, Cenozoic, Mesozoic (Jurassic and Triassic), and Permian sedimentary rocks down to 2507 m. The borehole section between 2411 and 2507 m below ground surface consists of a 'transition zone' containing siltstones and crystalline rocks. The composition of the granitic basement rocks range from hornblende-bearing, coarse quartz-rich biotite-granites at the top of the basement to monzogranites and more fine-grained monzonites with less quartz at deeper borehole sections (Käser et al., 2007). The granitic rocks have different types of high- and low-temperature hydrothermal alteration, such as the formation of Ca-Al-silicates (e.g., albite, epidote), anhydrite, calcite, and clay minerals (illite-muscovite and mixed layer smectite-illite). Käser et al. (2007) found several zones of argillic alteration and anhydrite, which they associated with cataclastic fracturing. The most prominent such zone extended between 4830.2 and 4835.6 m. Unfortunately, the orientation of these fracture zones could not be determined due to highly oversized borehole diameters making a proper analysis impossible with the acoustic borehole imager. The orientation of SHmax is NNW-SSE and nearly coincides with the azimuth of the dominant fracture set. The stress regime is predominantly strike-slip with relatively high deviatoric stresses following the hierarchy SHmax > SV > Shmin (Häring et al., 2008). The southernmost Upper Rhine Graben, including the Basel region, is situated at the junction between the Paleogene rift and the northern rim of the younger Jura fold and thrust belt that formed in Latest Miocene to recent times. The fault pattern in the Upper Rhine Graben at this location consists of three sets of faults striking NNE, ENE and NW that relate to the rift/graben structure, the Rhine-Bresse transfer zone, and the Variscian orogen, respectively. These basement fracture zones are prone to present-day activation by neotectonic activity (Ustaszewski & Schmid, 2007).

Reservoir temperature of the Basel-1 borehole was never measured before the hydraulic stimulation activities. The first temperature-log was run in December 2008, e.g. two years after the massive hydraulic injection test (Ladner & Häring, 2009), when the borehole was still producing intermittent outflow. The temperature-log reached a depth of 4600 m and ended 29 m above the casing shoe with a temperature of 173.6°C. Stober et el. (2022) estimated BHT of 185°C at 5 km through standard fluid geothermometer calibrations and extrapolations.

The result

The Basel-1 borehole was drilled to 5 km depth between May and October 2006, as the first hole of a doublet. The lowermost 371 m of Basel-1 was subjected to high pressure fracturing, injecting 11,570 m^3 with a maximum pressure of 30 MPa during 6 days in December 2006. The shape of the seismically active zone can be described as a near-vertical lenticular feature with an ESE offsetting branch and the seismically active volume is of the order of 35.000.000 m^3 (Häring et al., 2008). The injection was terminated after an earthquake exceeding ML 3 was registered, the largest event of ML 3.4 occurring shortly after closing the well (Deichmann et al., 2014; Ziegler et al., 2015). Due to the higher-than-expected seismic activity, and the reaction from the population, media, and the politicians, the experiment was stalled. Although the injected water was allowed to escape immediately after the mainshock and pressure at the wellhead dropped rapidly, the seismic activity declined only slowly, with three ML > 3 events occurring one to two months later (Kraft et al., 2009). Kraft el al. (2009) also conclude that the physical processes and parameters that control injection-induced seismicity - in terms of earthquake frequency, size distribution and

maximum magnitude - are poorly understood. However, many lessons have been learned from the Basel Deep Heat Mining Project:

- Before the well and stimulation process, Häring (2004) concluded that if induced fractures are observed in a balanced well, stimulation won't require large hydraulic pressures.
- Drilling problems in the sediments were caused by swelling clays and often led to stuck drill pipe. Problems were encountered in the crystalline basement as well.
- Because of the location of the wells under a city center, the potential for damage from a major seismic event associated with stimulation and production was greater than in rural areas.
- In order to create a larger "heat exchanger" volume in the subsurface, a sequence of parallel-trending reservoir disks might be developed by multiple injections at different levels in deviated wells. It is assumed that preexisting discontinuities strongly determine the reservoir geometry. Hence, additional targets may be identified by massive two- or three-dimensional VSP surveys from existing boreholes (Häring, 2008).

Pohang, South Korea (2010-2017)

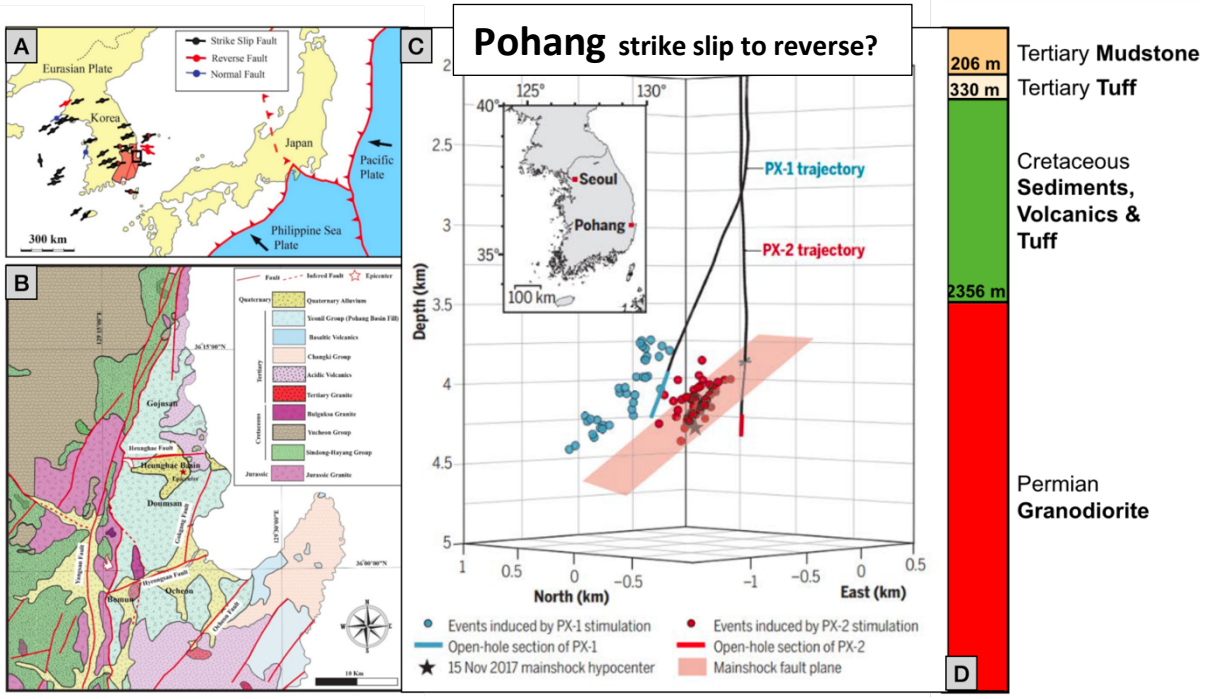

Figure 16. Pohang, Korea. A) Regional tectonic map of the study area. Bars indicate the maximum stress directions with major faulting type using past earthquakes of ML >3 and (B) shows a geological and tectonic map of the study area showing the epicentral location of the 15 November 2017 Pohang earthquake with major fault lines (from Naik et al., 2020). C) Showing the trajectories of the wells and the earthquake events occurred after and during the stimulation with the estimated mainshock fault plane (from Lee et al., 2019). D) Stratigraphy of the Pohang area (from Park et al., 2020)

Background

In 2010, the Korean government and the industry decided to invest in a 1.2 MW_{el} EGS power plant targeting 4-5 km deep granitic basement (Lee et al., 2015). The Pohang area (Figure 16) is one of the highest heat-flow (100-120 mW/m^2) areas in Korea and has been the focus of geothermal research since 2003. The Korea Institute of Geoscience and Mineral Resources performed a low-temperature geothermal development project in Pohang between 2003-

2008 including four exploration wells, the deepest reaching the granitic basement at 2383 m (Kim & Lee, 2007). Intensive geological and geophysical surveys such as airborne gravity, magnetic, radioactive, geochemistry and magnetotelluric campaigns have been performed to delineate possible fractures which can transport deep geothermal water to near surface. A low resistivity zone at depth disclosed a potential west dipping, hydraulically conductive fracture zone beneath the Pohang EGS site as a potential reservoir target (Lee et al., 2015). The temperature at 5 km depth of the Pohang area was expected to be about 180 °C based on a 1.5 km test-drilling (Kim & Lee, 2007).

Geology

Pohang is located in the Heunghae Basin, where a Tertiary mudstone and tuff layer >300 m thick sits on top of Cretaceous sediments and volcanic layer >2000 m thick. The top of the Permian granodiorite basement occurs at 2356 m (Figure 16D). The Korean Peninsula sits on the Eurasian Plate, whose tectonic activity is controlled by the ongoing subduction of the adjacent Pacific and Philippine Sea Plate and the collision of the Indian plate with the Eurasian plate (Figure 16A). Most of the Cenozoic tectonic deformation is accommodated by the two major fault systems, the Yangsan and Ulsan Faults (Figure 16B), along with crustal deformations along the eastern block of the Yangsan Ulsan Fault System. During the post Oligocene, the eastern block of the Yangsan–Ulsan Fault System drifted southeast and resulted in several NE–SW trending extensional faults with extensional basins. The epicentral area of the Pohang earthquake is one of those basins (Naik et al., 2020). Since the Pliocene Epoch, the regional stress field has changed from extension to compression, resulting in the reactivation of preexisting normal faults to strike-slip or reverse faults (Lee et al., 2015). However, as presented by Park et al. (2020), the tectonic regime and the stress at depth is not fully understood.

The result

Injection and production wells (PX-1 and PX-2) were drilled to 4,362 and 4,341 m with a bottom hole distance of 600 m and open-hole sections at 313 and 140 m respectively. Five hydraulic stimulations were conducted with a total injected volume of < 13 000 m^3 from January 2016 to September 2017 (Lim et al., 2020). Two months after the fifth hydraulic stimulation, the ML 5.4 Pohang earthquake occurred on 15 November 2017. After a year-long study, the government commission concluded that the ML 5.4 earthquake had been triggered by the hydraulic stimulations (Ellsworth, 2019). The project was suspended right after the ML 5.4 earthquake in 2017 and officially terminated in April 2019. Numerous studies are currently being conducted in search of causal linkages, triggering mechanisms, refined seismic analysis and lessons to be learnt.

- Prior to the injection, a mud loss event to the amount of 650 m^3 occurred during drilling of PX-2 in October–November 2015 at 3830-3840 m. Above, at 3790-3816 m, a fault zone with fault gauge containing breccia and cohesive cataclasite. The mud loss likely occurred in fractured host rock next to the fault zone (Ellsworth, 2019).
- In August 2018, wireline logging tools were deployed in PX-2 to image the borehole after the earthquake. The logging tools were unable to descend below 3,783 m due to obstruction of the well (Ellsworth, 2019).
- The 2017 Pohang and 2016 Gyeongju (40 km south of Pohang) main shocks, and their sequences, were similar in many ways. Both sequences were located in the vicinity of the Yangsan fault zone and had the same maximum magnitudes (McGarr, 2023).

- Comprehensive characterization of the faulting system and optimal well operation strategies are critical to mitigate potential seismic hazards associated with massive injection-extraction of fluids (Chang et al., 2020)
- In future EGS projects, the project team and the scientific institutions involved should engage in timely and adequate efforts to monitor, analyze and understand the evolution of any earthquake sequence, and provide information to the public authorities on the developing seismic risk conditions (Ellsworth, 2019).

Habanero, Australia (2002-2014)

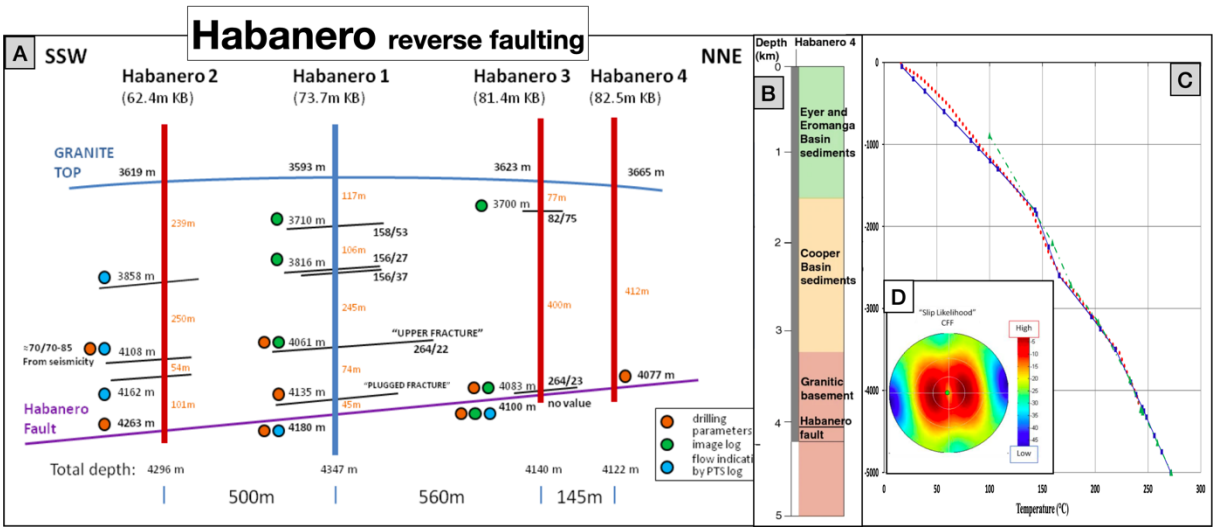

Figure 17. Habanero, Australia. A) The wells drilled into the Habanero fault zone. Note that the closed loop was between Habanero 1 and 4 only (from Humphreys, 2014). B) Simplified stratigraphy of the Habanero area (from Wang et al. 2022). C) Numerical estimate of the geothermal gradient and (D) SHmax orientation based on drill induced fractures (from Humphreys, 2014).

Background

Geodynamic Limited planned the Habanero Geothermal Project in the Cooper Basin in Australia to demonstrate the feasibility of an EGS in the high-temperature granitic basement, and planned to extend the demonstration site to produce hundreds of MW_{el} (Humphreys, 2014; Tester, 2006). The Cooper Basin was chosen from gravity modelling, due to the interpreted 1000 km^2 and 10 km thick heat-producing granite basement beneath the 3.5 to 4.5 km insulating sediments (Wyborn, 2010). Oil exploration encountered a 60°C/km gradient in the sediments and several wells intersected the top of the 220°C granitic basement (Figure 17A,C) (Humphreys, 2014). The Habanero Fault zone became the reservoir target after drilling the first well, Habanero-1 (Hogarth & Holl, 2017a).

Geology

The upper 1.3 km sedimentary cover of the Jurassic to Late Cretaceous Eyer and Eromanga basins, consists mostly of sandstones and fluvial deposits. The lower sedimentary cover, the intracontinental Carboniferous to Middle Triassic Cooper Basin sediments, is about 3.6 km thick and consists of glacial, fluviodeltaic and laucustrine sediments (Figure 17B)(Röth & Littke, 2022). The Cooper Basin contains the largest on-shore accumulations of oil and gas in Australia and Cretaceous volcanic activity is suggested to have caused a thermal anomaly (Wyborn, 2010). Below is the Permian (320 Ma) basement of the Innamincka granite (Figure

17B), a coarse-grained, white, felsic syenogranite containing quartz, perthitic microcline with subordinate plagioclase, and former biotite which has mostly been altered to chlorite (Röth & Littke, 2022). After seven decades of exploration, various uncertainties remained concerning the formation of the Cooper Basin (Röth & Littke, 2022). The regional stress is related to thrusting and has been for the last 5-15 Ma. The minimum stress is therefore lithostatic pressure (Sv) (Wyborn, 2010). The presence of a large granitic body with relatively high abundances of radiogenic elements is suggested to have heat productivity in the range 7-10 $\mu W/m^3$ (Wyborn, 2010) and 3.5-14.5 $\mu W/m^3$ (Humphreys, 2014). However, no data on the average RA element proportions have been published.

The result

The first well, Habanero-1, was drilled from February 2003 to October 2003 (241 days) reaching a depth of 4253 m, where it intersected the main fracture. After completion, the well was stimulated with total 20000 m3 water causing 28,000 microseismic events in an area of 2.5 km^2 (Humphreys, 2014). In July 2004 to January 2005, Habanero-2 was drilled to 4358 m. There were several challenges, especially when entering the main fracture where 4 sidetracks were drilled but were ultimately unsuccessful in establishing connection to the main fracture, hence drilling was suspended. In response to the host of drilling problems of Habanero-2, Geodynamics bought their own drilling rig. Habanero-3 was drilled September 2007 to February 2008 (147 days) to 4221 m using a Managed Pressure Drilling technique and successfully drilled into the Habanero Fault. In March 2008, they opened the well to fluid flow and reached 207°C at 16.5 l/s. Circulation tests with Habanero-1 achieved a flow rate of 18.5 l/s at injection pressures of 51 MPa. They traced the mean residence time to 23.7 days and 78% of the tracers was returned. The casing failed near the surface due to caustic stress corrosion cracking in the annulus of the drill hole. The casing in the top 6 m of the well ruptured with water and steam flowing from the well for approximately 25 days before it was controlled (Humphreys, 2014). In March to September 2012 (200 days), the most successful well Habanero-4 was drilled to 4225 m. The partners spent AU$9 million on the design of Habanero-4 to mitigate all of the issues encountered in the previous wells. In the later part of 2012 Geodynamics conducted further hydraulic stimulation and flow testing from Habanero-4 and achieved the highest ever open-well flow rates from an EGS well. Geodynamics successfully commissioned the 1 MW_{el} pilot power plant in the second quarter of 2013 using Habanero-1 as injector and Habanero-4 as producer (Figure 17A). It was successfully producing 19 l/s and 215°C through a closed loop for 160 days, generating electricity to power the re-injection pump, the site camp and all other ancillary loads.

Despite these technical successes, the project failed to satisfy key economic measures and the entire project is in the process of being abandoned (Hogarth & Holl, 2017b).

- The high fluid pressures required changes to the drilling configuration (use of heavy mud rather than water in order to control the overpressures). This led to a doubling of the original budget (Humphreys, 2014).
- During mid-2009 Geodynamics successfully achieved closed-circuit flow between Habanero-1 and Habanero-3, a very significant technical win. Within a week prior to connecting the flow circuit to a 1 MW_{el} generator, the steel casing in the upper part of Habanero-3 cracked. A detailed investigation determined that an incomplete cement job left an air pocket between the steel casing and the rock formation (Humphreys, 2014).

- Two electromagnetic surveys were undertaken by researchers from Japan but neither survey was able to provide additional information about the Habanero reservoir (Humphreys, 2014).
- The mineralogical composition of cuttings does not change significantly near and at the Habanero Fault intersection. If there is any kind of fault gouge present then the cuttings were probably broken down during the transport to the surface.
- In their internal report, Geodynamics Ltd. conclude there is currently no technology available that can remotely identify and locate existing faults in granite rocks. Drilling is the only option, which leads to higher exploration risks for future EGS projects (Humphreys, 2014).

United Downs, United Kingdom (2009-present)

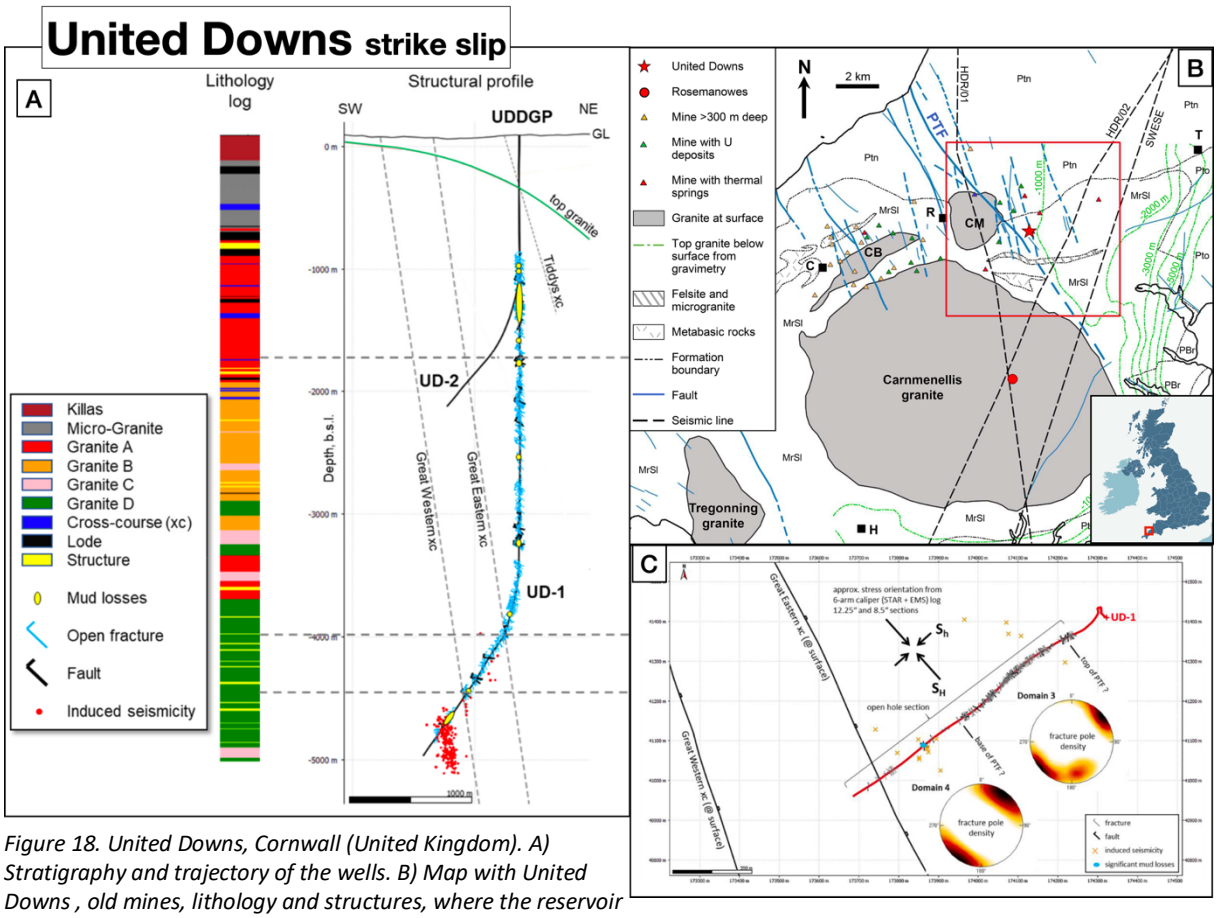

Figure 18. United Downs, Cornwall (United Kingdom). A) Stratigraphy and trajectory of the wells. B) Map with United Downs , old mines, lithology and structures, where the reservoir target Porthowan fault is abbreviated PTF. C) Map of the UD-1 trajectory and its orientation normal to the SHmax (from Reinecker, 2021)

Background

The United Downs Deep Geothermal Power Project (UDDGP) was initiated in 2009 by Geothermal Engineering Ltd with the goal to establish geothermal power production in the UK. It is funded both by public and private sector (Reinecker, 2021). The reservoir target is the 200-500 m wide, subvertical, strike-slip Porthowan Fault (Figure 18), aiming to produce 1-3 MW_{el} with fluid flows of 20-80 l/s (Ledingham et al., 2019). It has been known for decades that the heat-producing granites of SW England represent a potential geothermal

resource. Heat flow in the Cornish granite is approximately double the UK average, at more than 120mW/m^2. The records from mining activity in the United Downs area, although >100 years old and only covering the top 400 m of the 5 km deep drilling prognosis, provides important data on fault dip, dip direction, displacement, infill, and thickness (Le Boutillier, 2002). This, together with the surface geological maps, were used to develop the conceptual fault model and prepare the drilling prognosis. Furthermore, heat flow studies and geothermal assessments carried out in the 1970s to the early 1990s in Cornwall were at the forefront of EGS research through the Rosemanowes geothermal research project (Parker, 1999; Tester, 2006). One of the surprising outcomes of that work was that injected water migrated downwards by shear stimulation on favorably oriented joints but, as a result, a significant percentage of the injected water was lost (Parker, 1999; Reinecker et al., 2021). In the UDDGP, they assumed similar SHmax orientations and therefore planned the injection well above the production well. The aim was to have a large distance between the wells to create a large volume reservoir. The main risk was to not reach sufficient fluid flows in the Porthowan fault zone at depth (Reinecker et al., 2021).

Geology

Most of the Cornish geology is comprised of Devonian metasedimentary rocks, "killas", and the Early Permian "Cornubian" granite batholith. During Devonian extension, basic igneous rocks intercalated as sills or layer-parallel bodies. This succession was intensely affected during Variscan orogeny (mainly thrust faulting, folding and low-grade metamorphism) (Warr et al., 1991). The Cornubian granite formed during the late stages of the Variscan orogeny in the Early Permian (c. 280 Ma) and its RA heat production coupled with a deep, permeable fracture system, has been suggested to be the main cause of the thermal anomaly in SW England (Parker, 1999; Tammemagi & Wheildon, 1977). The extent of the Cornubian granite is estimated by gravity and seismic modelling to have an average thickness of between 3.7 km and 10 km (Reinecker et al., 2021 and references therein). The Porthowan Fault is a >15 km long NNW-SSE oriented strike-slip fault zone 200-500 m wide (Figure 18B). It belongs to a family of similar structures that accommodated the oblique closure of the Variscan orogenic belt in southwest and southern England (Reinecker et al., 2021). Stress orientation derived from borehole breakouts and drilling induced tensile fractures observed in the ultrasonic image log of the 12.25" section in UD-1 shows SHmax azimuth of 134° (Figure 18C) (Reinecker et al., 2021).

The result

In 2018-2019 two wells, UD-1 (production) and UD-2 (injection), were drilled using a conventional rotary technique to a TVD of 5053 m (161 days) and 2214 m (49 days) (Ledingham et al., 2019). Throughout 2020 and early 2021, the wells underwent significant testing and hydraulic stimulation whereby water was injected at varying volumes and flow rates into both wells to assess and develop the hydraulic properties of the deep reservoir. Shortly after flow-testing operations began in August 2020, a series of induced seismic events, with a maximum magnitude of 1.7 and a maximum intensity level 3 (i.e.- weak vibrations) occurred (Rodríguez-Pradilla & Verdon, 2021). The project reached an important milestone at the beginning of July 2021, when an Electrical Submersible Pump (ESP) was lowered to a depth of approximately 1 km into UD-1, and coupled to injection pumps on UD-2 to simulate power plant operation and test the performance of the whole reservoir. It was successfully installed, and the UK's first geothermal steam was produced. The ESP was run

over a seven-day period (Farndale & Law, 2022). The seismic network is used for delineating the growing reservoir, enabling the calculation of a minimum estimate for the reservoir volume of 50,900,000 m^3 (Farndale & Law, 2022). Testing and hydraulic stimulation has been undertaken and the installation of a c. 3 MW_{el} power plant is set to begin in late 2023 (*pers comm.* K. Mallin).

Espoo, Finland (2014-2022)

Background

The aim of the St1 Deep Heat Project was to build a pilot EGS to explore the technical and economic feasibility of deep geothermal energy extraction in the crystalline basement of Finland for production of thermal power to a district heating network (I. T. Kukkonen & Pentti, 2021). Due to the demands from Fortum, the district heating owner hence the consumer, the target was to produce hot fluids at about 100°C and re-inject it to the formation at 50°C (Karlsson, 2022). The 100°C goal requires a >6 km deep reservoir due to the assumed geothermal gradient of 17 °C/km (I. T. Kukkonen & Pentti, 2021). The drill site is located in Espoo, next to the Fortum district heating plant on the Aalto University campus. The goal was to reach 40 MW_{th} with temperatures of >100°C and fluid flow of at 50 l/s to supply 10% of the district heating system in Espoo (Karlsson, 2022). This is the deepest EGS initiative in the world so far.

Geology

The drill site geology is typical for the south-central part of the Fennoscandian Shield, where a 10 m layer of Quaternary sediments overlies the Precambrian bedrock. The bedrock comprises c. 1.8 – 1.9 Ga old migmatitic rocks, i.e. mixtures of veined gneiss, mica and hornblende gneisses, amphibolite and granitic intrusions (Figure 19C). The lithological boundaries are mostly steep and subvertical. Due to extensive deformation and migmatization during the geological history of the area, the target formation structure is complex (Kukkonen et al., 2023). At the surface level, there are several km long linear structures on topographic, geophysical, and geological maps (Heikkinen et al., 2021).

In an internal report, Backer and Meier (2016) estimate SHmax from borehole breakouts in OTN-1 to have an azimuth of 108°, where the SHmax > Sv > Shmin implyies a strike-slip regime. However, through extrapolation of the stresses and their vertical gradients determined in the testhole between 700-1720 m, thrusting is believed to occur at shallower levels and strike-slip faulting below 1-2 km (Kukkonen et al., 2023).

The result

A cored TVD 1956 m testhole (OTN-1) was drilled in 2015 to provide baseline information of the rock types, temperature gradient, geophysical properties, and stress field (Kukkonen et al., 2023). After drilling, the hole was utilized for seismic observations with a downhole array in the first well (Heikkinen et al., 2021). Drilling of the deep well (OTN-2) was started in May 2016. Air hammer drilling was used from 296 m to 3300 m (reached in August 2016). The drilling of OTN-3 started in August 2016, with air hammering between 300 m and 3300 m, thereafter rotary drilling was used to 6400 m, reached December 2017 (150 days) (Kukkonen et al., 2023). Water hammer drilling was tested from 3300 m, but did not prove to be technically reliable, and the final deepening and deviation of the OTN-2 from vertical was done with rotary drilling from January to May 2020 (Kukkonen et al., 2023). With this drilling strategy, a VSP array was recording from OTN-1 while OTN-2 was being drilled, using the

hammer as a seismic source. The same strategy was to be carried out between OTN-3 and OTN-1 but unfortunately, OTN-1 was damaged due to a technical error in the drilling operation and a new array was ordered to be used in OTN-2 (Heikkinen et al., 2021). When that array arrived, the air hammer was however replaced by rotary drilling for constructing the deviated bottom section of OTN-3, making it unable to cause enough seismic noise (Heikkinen et al., 2021). A VSP survey was carried out in OTN-2 in 2016 and data was collected at 2000-4000 m (Heikkinen et al., 2021). The VSP results revealed an ENE, 70° dipping reflecting zone, which coincides with the 45° dipping, 70-80 °

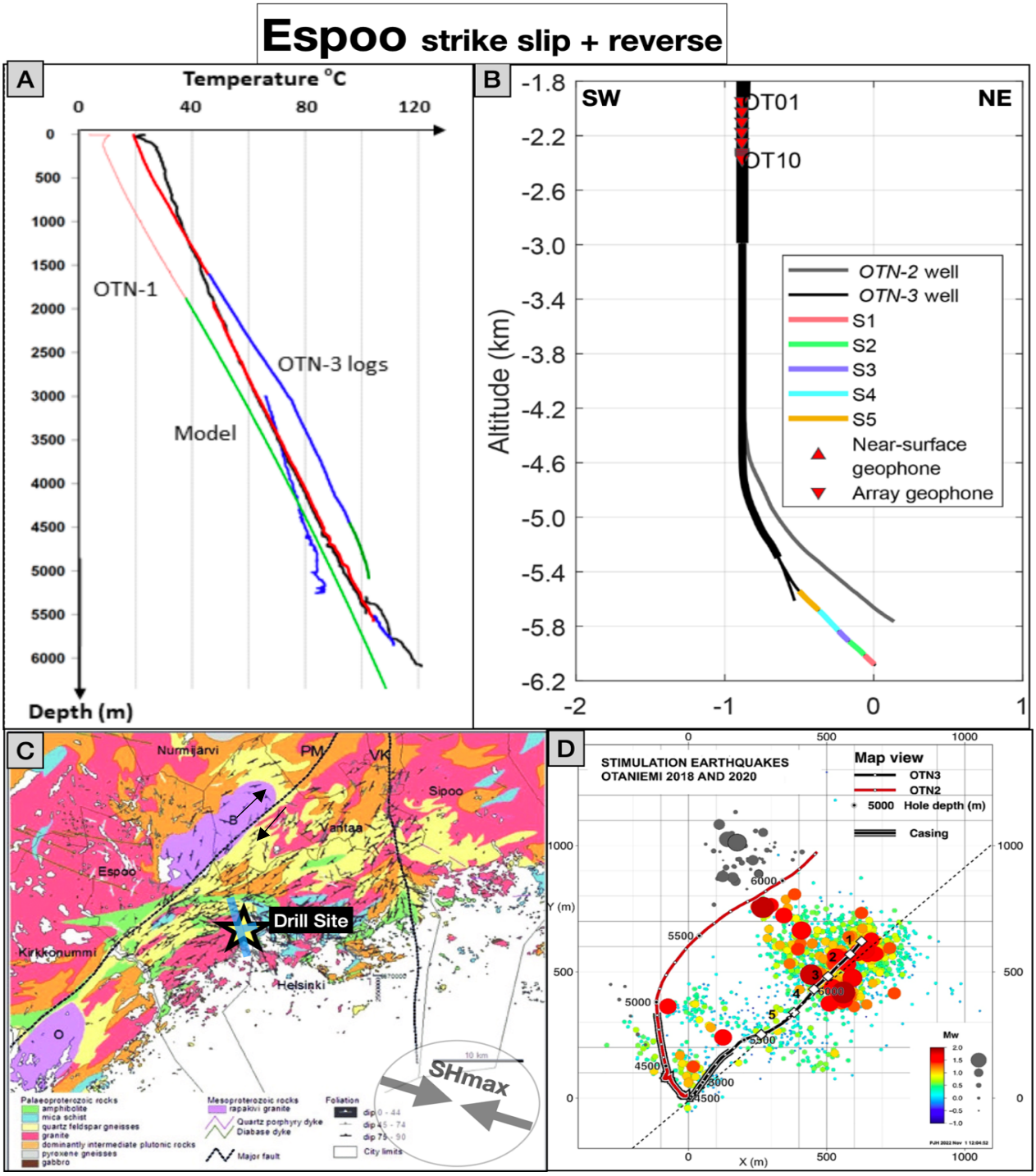

Figure 19.Espoo, Finland. A) Geothermal gradients in Espoo (from Kukkonen & Pentti, 2021). B) The design of the well from Leonhardt et al.,(2021);view in azimuth 40° (approximately SW-NE). C) Geological map of Helsinki area from Airo et al. (2008) with the location of the drill site from the Espoo project; the blue marker shows the dip direction of the 45° dipping, 300-400 m fault zone encountered at 4.5-4.9 km (from Heikinen et al., 2021) and SHmax (from Kukkonen et al., 2023). The shear sense for the Porkkala-Mänsälä (PM) structure is inferred (Pajunen, 2008). D) The seismic cloud from a map view (from Kwiatek et al., 2022).

azimuth, 300-400 m fracture zone encountered at 4.5 km in OTN-3, suggesting it to be a listric fault (Figure 20) (Heikkinen et al., 2021).

The stress field data suggest that vertical fractures and WNW – ESE faults are optimally oriented for hydrofracturing at a target depth of 5 - 7 km. Consequently, the deviated parts of OTN-2 and OTN-3 were directed to NNE (azimuth 32 - 39◦).

In June and July 2018, a total of 18,160 m^3 of water was pumped OTN-3 the rock formation at true vertical depths of 5.7 to 6.1 km over a period of 49 days with maximum pressures of 90 MPa (Kwiatek et al., 2019; Leonhardt et al., 2021). The average natural permeability derived from leak-off tests and well tests before stimulation and from cross-hole pressure data is $1\cdot 10^{-17} – 1\cdot 10^{-16}$ m^2, which agrees with permeability models for the brittle crystalline crust at this depth. Hydraulic stimulation increased permeability to $10^{-13} – 10^{-12}$ m^2, but it gradually decreased back to the natural levels after pressure release (Kukkonen et al., 2023). Stimulation generated five micro-earthquake clusters at 4.8 – 6.3 km TVD depth spatially presented in Figure 19D. Hydraulic connections between clusters were

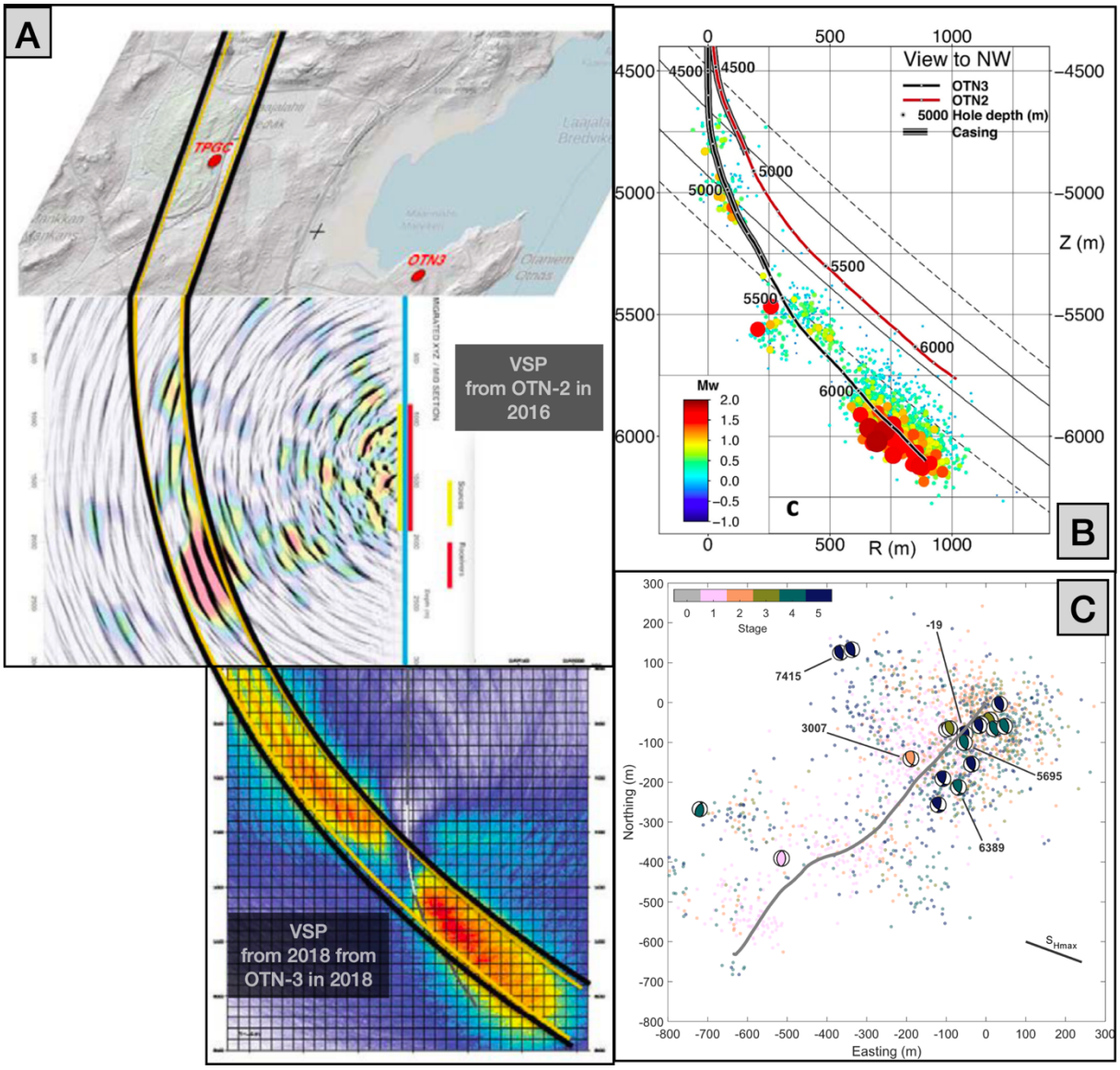

Figure 20. A).Interpretation of fracture zone from the VSP survey in 2016 and 2018 (Heikkinen et al., 2021). B) boundaries of the reflecting zone with the 2018 and 2020 stimulations (from Leonhardt et al., 2021). Dashed lines show the boundaries of the low velocity zone, and the solid lines the heavily fractured zone, respectively. C) Focal measurements of the largest seismic events (from Holmgren et al. 2023).

apparently not attained (Kukkonen et al., 2023). Holmgren et al., (2023) contributed with focal interpretation from the seismic cloud, showing an unexpected rupture growth of oblique reversed faulting (Figure 20C).

The project generated extensive experience and data sets regarding deep drilling, hydrogeological properties, and seismic response to stimulation of crystalline rock in the upper continental crust. Hydraulic conductivity turned out to be the most challenging issue for the St1 EGS project which is not continuing at the moment (Kukkonen et al., 2023). The St1 Deep Heat Project with its two deep wells extending to 6.2 - 6.4 km depth is the world's deepest industrial geothermal energy project to date.

Lund, Sweden (2001-2003)

Background

In 2001, Lund Energi AB (now Kraftringen) and Lund University launched a geothermal exploration project in Lund. The aim was to find >100°C water for the district heating system, targeting the fractured granite in the Romeleåsen Fault Zone. The geological model of the Romeleåsen Fault Zone and the well site is based on bedrock maps, seismic investigations, aeromagnetic data, and gravimetrical data, as well as regional tectonic studies of the Sorgenfrei–Tornquist Zone and the Fennoscandian Border Zone (Rosberg & Erlström, 2019).

Geology

At about 2000 m depth, the Precambrian basement starts, here as various gneisses, granite, amphibolite, metabasite and dolerite. The gneisses have ages of about 1700 Ma, the metabasite 1200–1700 Ma, and the granites about 1450 Ma. The dolerites are related to two different dyke systems, one c. 930–1130 Ma old running NNE–SSW and a younger c. 290–300 Ma old system running NW–SE (Rosberg & Erlström, 2019). It is covered by a Triassic to Paleogene sedimentary succession including claystone, sandstone, limestone, arkose and coal. On top of that, a Quaternary till/sand cap is covering the upper meters (Figure 22). The province of Skåne lies in the complex buffer zone between the stable Fennoscandian Shield to the north and younger tectonic regimes to the south, resulting in a complex subsurface geology across the Sorgenfrei-Tornquist Zone which formed in the Late Palaeozoic (Rosberg & Erlström, 2019). The Sorgenfrei–Tornquist Zone in Skåne is a deep-seated, NW–SE-oriented fault zone that was reactivated during Mesozoic rifting and thrusting.

The result

A BHT of around 85°C (Figure 21) and insufficient permeability made a commercial geothermal system unviable, according to the investor. Four different drilling methods were used: conventional mud rotary drilling, air rotary drilling, percussion drilling using air, and percussion drilling using mud. Conventional mud rotary drilling was used in the sedimentary succession as well as in parts of the crystalline basement, while the other methods were only applied to the crystalline basement. At 3365 m, the drill string got stuck which required cutting off the drill string assembly. Furthermore, the seismic reflectivity of the crystalline basement is poor. Scattered discontinuous sub-horizontal reflectors were interpreted to represent occurrences of bodies and dykes of metabasite and dolerite and the basement faults were poorly seen in the seismic data. Therefore, the deeper configuration of the Romeleåsen Fault Zone in the Lund area is not well-defined by the seismic survey (Rosberg &

Erlström, 2019). The heat productivity in DGE-1 is, overall, relatively high with an average of 5.8 µW/m^3, which might be the reason for the relatively high geothermal gradient in the basement (Figure 21). One experience from the DGE-1 exploration project is that cores are necessary, at least over parts of the target section, to perform a proper classification and characterization of the rock mass and fracturing characteristics. It is also a necessity to have cores for determining hydraulic and thermal properties of the crystalline bedrock. A lesson learnt is that results from a density log are required to achieve a better calculation of the heat production. The quality of the evaluation of the thermal properties would improve if these sources of information were available (Rosberg & Erlström, 2019).

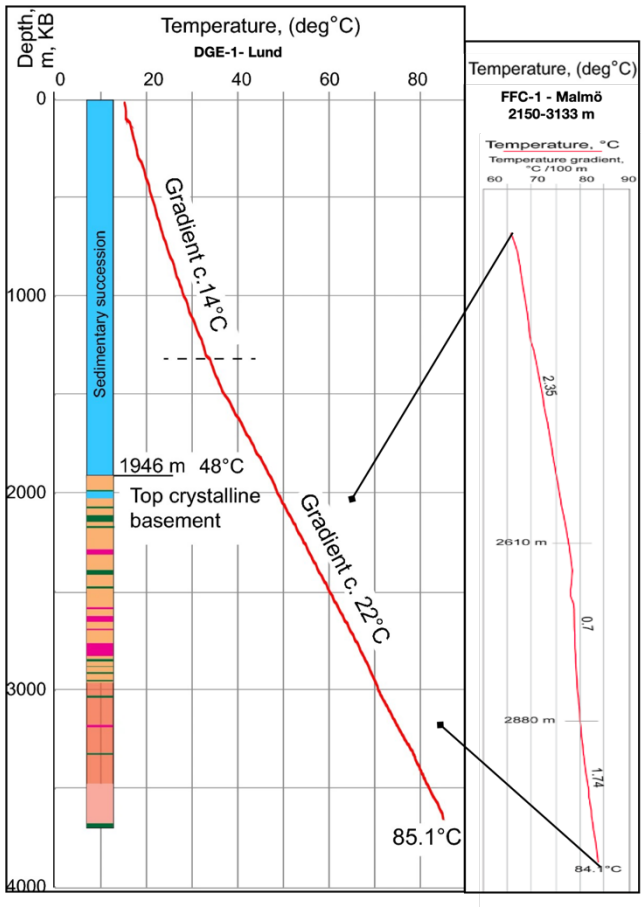

Figure 21. Stratigraphy and geothermal gradient from DGE-1 in Lund to the left compared and the geothermal gradient from the last part, 2150 m to 3133 m of FFC-1 in Malmö (from Rosberg & Erlström, 2019)

Malmö, Sweden (2003-2004 and 2016-2020)

Background

In 2002-2003, Sydkraft AB, today E.ON, drilled two wells in the sedimentary layers in Malmö to 2150m. This project was terminated for economic reasons, but flow tests showed a possible production of 10 MW_{th} (Energimyndigheten, 2021). In 2016, the ST1 project in Finland triggered E.ON to investigate the potential for EGS as a future sustainable heat source for the Malmö district heating system. The goal was to explore thermal and hydraulic properties, fracture zones, stratigraphy, structures and drilling conditions at 5-7 km with BTH of 160°C to produce 50 MW_{th} for the district heating network. The final goal was to make five EGS facilities around the city (Energimyndigheten, 2021).

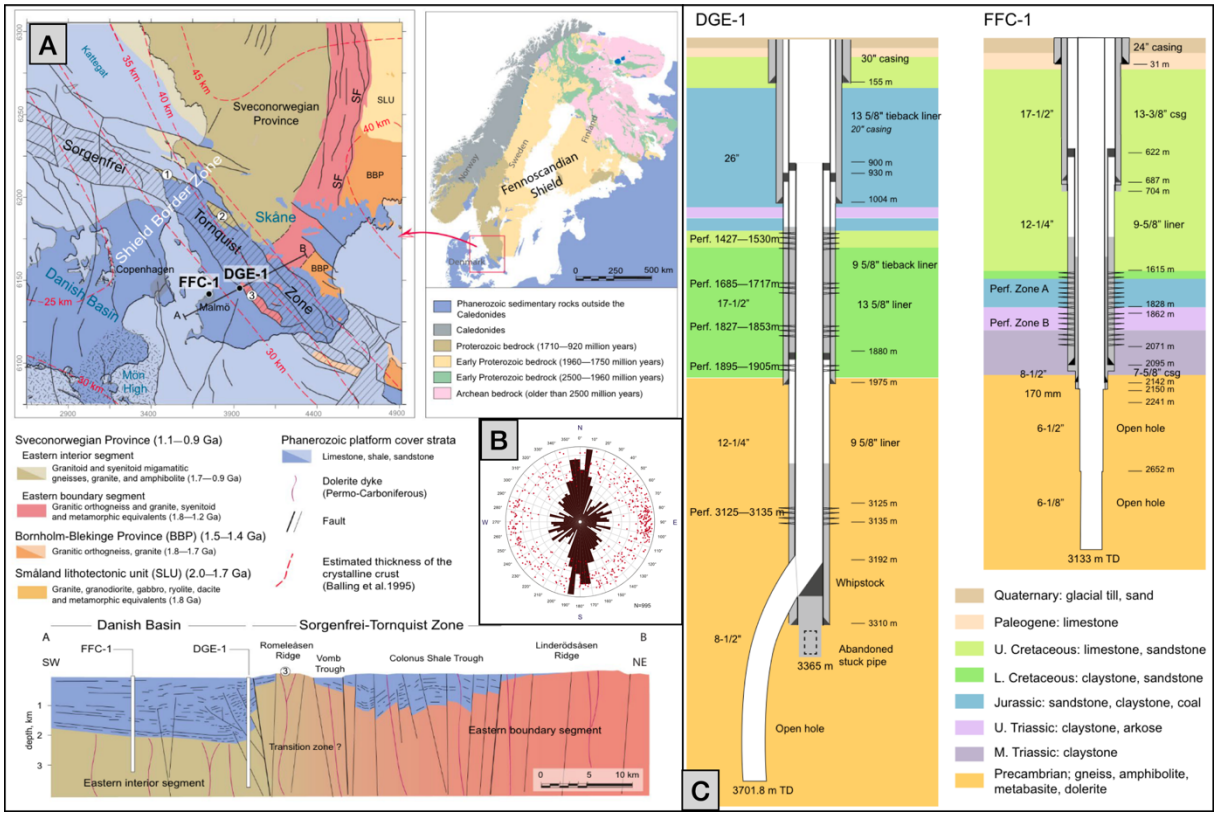

Figure 22. A) Geological setting of the southwestern part of the Fennoscandian Shield and the location of the DGE-1 (Lund) and FFC-1 (Malmö) wells (from Rosberg & Erlström, 2021). B) Fractures in interval between 2,366 and 3,106 m in FFC-1 indicating a SHmax orienting S-W (from Juhlin, 2022). C) Schematic description of DGE-1 (Lund) and FFC-1 (Malmö) (from Roberg and Erlström, 2021)

Geology

The stratigraphy is basically the same as in Lund (Geology). But here, the upper c. 400 m of the basement in FFC-1 is severely fractured and water-bearing. From drill induced fractures, the direction of the maximum horizontal stress at about 2,500 m depth is N–S to NNE–SSW (Figure 22). The average heat production is 3.0 µW/m^3 in FFC-1. The rocks in FFC-1 are depleted in uranium and thorium in comparison to the rocks in the DGE-1 borehole (Rosberg & Erlström, 2021). The gradient in the crystalline basement was in the order of 17.4 °C/km (Figure 21). Above, a very low gradient of 7 °C/km was encountered in a 270 m interval (Figure 21) suggesting convective mixing in this zone (*pers comm*. M. Erlström).

The result

The drilling exceeded budget and was stopped at 3133 m (Energimyndigheten, 2021). They started with air DTH drilling technique, using the same company as in Espoo, but the water inflow was too high and they had to change to the more slow and therefore more expensive rotary drilling (*pers comm.* J. Rosberg). The lack of a clear top-of-basement reflection is judged to indicate that the uppermost crystalline basement is highly fractured; this point was not stressed in the pre-drilling stage, which could have guided the choice of drilling technology and potentially saved significant costs to the project (Juhlin et al., 2022). Potential steeply dipping fracture zones can be inferred from offsets in the sub-horizontal reflectivity or by near-vertical transparent zones, but any such interpretations should be treated with caution (Juhlin et al., 2022). The SHmax orientation (Figure 22B) is inconsistent with that expected from the regional stress field based on seismicity studies in the area with

a maximum horizontal stress in the NW –SE direction. Still, the unexpected N–S orientation give an unique insight to that the stress situation on the margins of the FSS, which is more complex than anticipated (Juhlin et al., 2022). Juhlin (2022) conclude that this unexpected SHmax orientation demonstrate the importance of in-situ measurements of the stress field to understand the expected response of the rock mass to stimulation.

Discussion

Synthesis

The evaluation of the deepest EGS projects in crystallin rocks has shown how deep geothermal energy in unconventional geological settings has been successful in three of eight projects (assuming United Downs will commence). This study also shows how and why five of them failed. All EGS projects in this study have failed with reference to commercial profitability. However, all projects may be regarded as demonstration/or pilot projects partly funded by governments, hence profitability is intended for later efforts based on what has been learned from these examples.

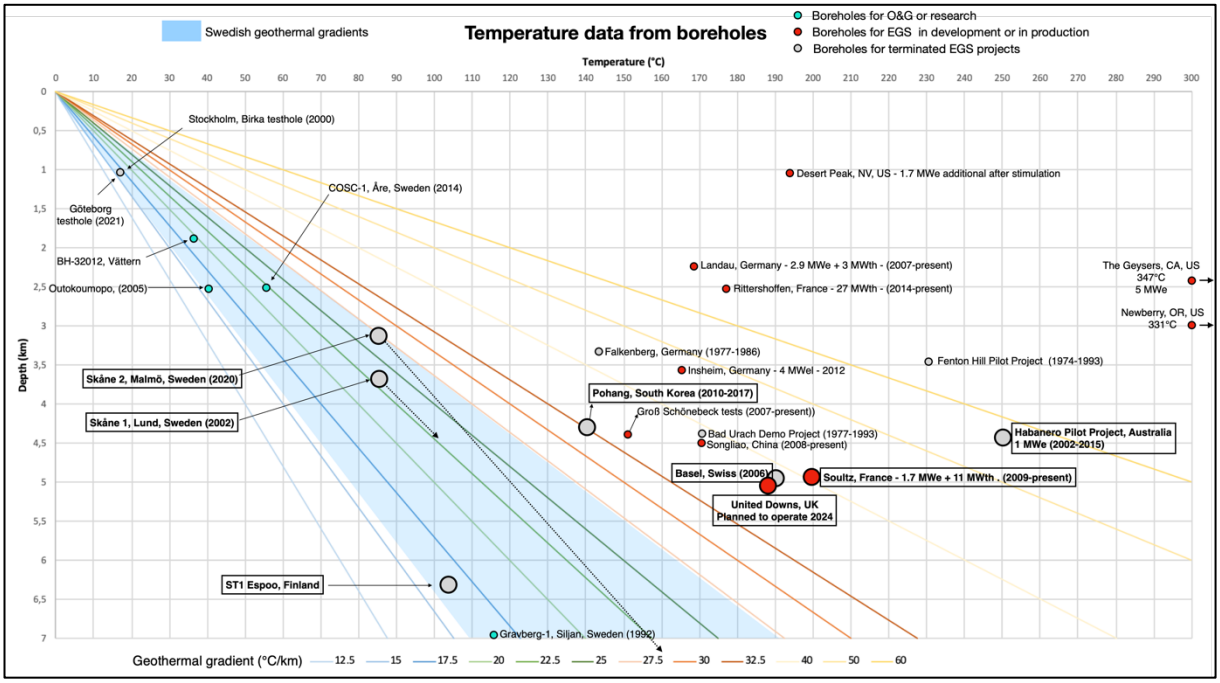

Figure 23. The BTH data from the case projects along with other EGS projects throughout the world, plotted in linear average geothermal gradients. The arrows from the two Skåne projects show the minimum depth to reach the project temperature goal, based on assumed liner geothermal gradients in the crystalline basement. The values from the other EGS projects are compiled by Li et al. (2022) and for the Swedish and Finish boreholes, see Table 3 in Rosberg & Erlström (2019) and references therein. For the others, see result section in this report.

Table 4 show how far each of the eight projects came with reference to each other in simplified stages typically executed in EGS projects. In Habanero and United downs, there were no testholes, but they had mining or O&G exploration boreholes in the near vicinity, hence they had enough thermal and structural data to make a conceptual model. All projects had some kind of conceptual model. However, the resolution and credibility vary significantly. In Lund, the conceptual model was only based on geophysics and structural interpretations. The most detailed conceptual model was for United Downs where a specific

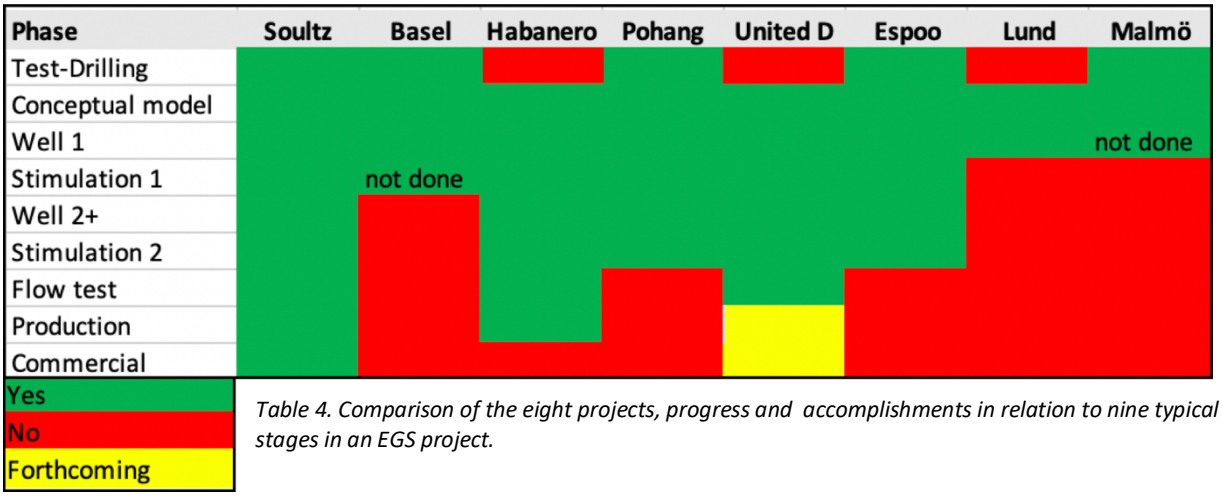

Table 4. Comparison of the eight projects, progress and accomplishments in relation to nine typical stages in an EGS project.

and described structure, the subvertical strike-slip Porthowan fault zone, is perfectly parallel with the SHmax making the well design geometrically straightforward pre-drilling. Here, the mining history in combination with the Rosemanowes geothermal testing program in the 1980s contributed with vital subsurface data to develop this clear conceptual model. The main question was whether fluid flow would make it all the way down to 5 km. Therefore, they set a humble goal of 1-3 MW_{el} and fluid flows between 20-80 l/s. The other projects had a set MW goal. None of the other projects presented a detailed concept of a reservoir target beyond the extrapolated thermal and SHmax data from the testhole. The reservoir would rather be determined during the well drilling process, depending on the stress field based on drill induced fractures and encountered fracture zones. One could easily argue that Basel, Espoo, Lund and Malmö had unrealistic output expectations from the initial stage based on what was achieved before. For example, Malmö sought 160°C at c. 7.5 km, which is unrealistic assuming a linear geothermal gradient of 17.4°C for the crystalline basement (Figure 23). However, the geothermal gradient at the basement was unknown at the time they set their goals.

All projects managed to drill at least one well. In Malmö, however, they decided to cancel before they reached their target depth. For completed projects, available starting dates and an ending dates of the drilling was gathered, making it possible to compare the unbiased total drilling times for each project (Table 5) without consideration for ROP or other external obstacles. The comparison reveals that the fastest drilling occurred in Espoo, averaging 2.2 m/h. The reason for this result is the use of the DTH hammer, which was successfully used to

	Basel	Habanero	Pohang	United Downs	Espoo	Lund
Mean drilling time Well 1	1,16	0,75	0,65	1,37	1,73	1,05
Mean drilling time Well 1		0,86	0,32	2,03	2,67	
Mean drilling time both wells	**1,16**	**0,81**	**0,48**	**1,70**	**2,20**	**1,05**

Table 5. Showing the average drilling times for all projects but Soultz and Malmö.

a depth of 3300 m for both wells. Pohang had the slowest drilling time, averaging 0.48 m/h (Table 5). To evaluate the best drilling strategy, the operational drilling parameters need to be assessed in detail.

$$\frac{\text{Measured depth (m)}}{\text{Drilling days} * 60} \qquad \textit{Equation 5}$$

Structure geometries and well orientation

In Espoo, the first VSP (in 2016) detected the ENE (70-80° azimuth), 70° dipping fault zone, but only down to 4000 m (Figure 20A) (Heikkinen et al., 2021). Whether the plan at this time was to target the zone as a reservoir or not is unclear. However, they hit the zone and deviated the well into the zone at 4.5 km (Figure 20B), here dipping only 45°, indicating a listric shape of the fracture zone (Figure 20A). This structural and geometrical relationship is not ideal for hydro shearing due to the orientation and dip angle of 45° in the reported stress field for two reasons: (1) If the tectonic regime is strike-slip, a subvertical (strike-slip) structure striking in SHmax should be targeted (Figure 24A). (2) If the tectonic regime is compressional, which is partly suggested for Espoo, the fault plane should be dipping perpendicular to SHmax, which is not the case (Figure 24B). However, an oblique strike-slip transpressional regime might fit perfectly with the direction of the NE dipping listric fault (Figure 24C). But is a listric fault usually reactivated in an oblique strike-slip transpressional regime? It raises the question whether the propagation of stimulation is controlled by the in-situ stress or the fracture zone? Usually, fracture zones are defined by the current stress field, and for Espoo this zone might be included in some extensional deformation (transtension) related to the sinistral strike-slip Porkkala-Mäntsälä shear zone about 7 km NW of the site (Figure 19A). This might be consistent with a listric shaped normal fault associated with extensional regimes (Figure 24D). This theory would strengthen the argument by Juhlin et al. (2022) of unpredictable stress orientations as transpression/transtension both occur along strike-slip faults, hence measuring the in-situ stress is of great importance. These geometrical uncertainties complicate the important decision of how to orient the wells.

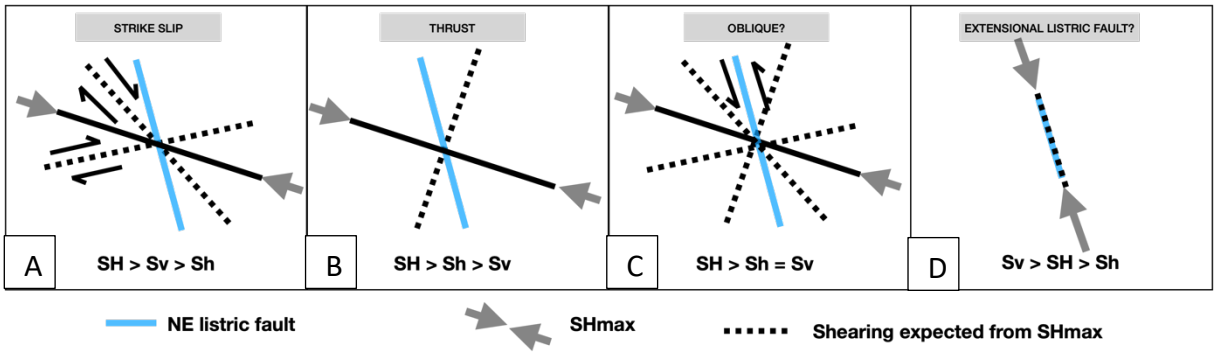

Figure 24. Simplified visualization of expected shearing from four different tectonic regimes acting on the ENE dipping listric fault in Espoo. Reported stress field is 110° (WNW-ESE). An oblique strike-slip transpressional regime might agree with shearing, but the listric shape of the fault might be problematic. A potential extensional regime is based on interpretation that its a listric fault and its relation to the sinistral Porkkala-Mäntsälä shear zone 7 km NE of the drill site.

The distance between the production and injection well is 600 m for Soultz and Pohang, 705 m for Habanero and 400 m for Espoo. In United Downs, it is 2000 m. A long distance between the wells, by definition, increase the chances of having a large reservoir

volume. However, the possible distance is determined by the permeability. The permeability is determined by the stimulation results which is partly spatially indicated by the propagation of the seismic cloud. In Soultz, two injection wells were drilled, but one of them (GPK-4) lost almost all the injected fluid. The permeable fracture network is not fully understood here, despite plenty of research through microseismic imaging, stimulation and flow tests. In Espoo, one can see that the seismic cloud was close to the well (Figure 19D, 20B,C). This gives an idea of a suitable distance between the wells. Maybe 400 m was too much in Espoo or, was the second stimulation expected to propagate towards the first well, but instead it propagated away from it, towards NW (Figure 19D)?

The triggered seismicity issue

The lessons from Pohang and Basel are numerous. Both projects neglect the avoidance of near-critical stressed faults, i.e.- naturally seismic active zones. The devastating Basel earthquake of 600 years ago is well known and in Pohang, the > M 5 earthquake along the active Yangsan Fault 40 km to the south, occurred c. one year before the stimulation process in 2017 (Figure 16). In Basel, they aimed for the largest "Main boundary fault" (Figure 15). In the open hole section they encountered two large catalasite zones with no orientation data. Such zones should be fully understood to plan for optimal and safe stimulation. In Pohang the structure that caused the large mud-loss during the drilling of PX-1 (Figure 16) which was later determined to be responsible for the earthquake, should obviously have been characterized, since it was dipping straight into the intended reservoir target zone. The potential length of the fault zone that were encountered in combination with their potential near-critical slip rates suggest that low pressures associated with the hydraulic stimulation could be enough to induce shearing. They injected 11500 m^3 in Basel and 13000 m^3 in Pohang with maximum pressures of c. 30 MPa and 90 MPa respectively. In both cases, had a more proactive understanding of the fault slip tendencies, their orientation and extent, along with a more sensitive TLS assessment been undertaken, a different stimulation strategy might have been considered, i.e.- lower pressure over longer times with a high resolution microseismic observation system to analyze the propagation of the reservoir and the intensity of the seismic activity. In the case of Pohang, they probably would have reconsidered the arrangement of the wells if they had more structural insight. The best would be if all structures intended to be stimulated were described in a Mohr diagram to control the stimulation. Therefore, in-situ stress measurements with orientations and magnitudes are preferable, along with the slip tendency estimations for the structures intended to be stimulated. In this case, all structures intended to be stimulated can be assessed in a proactive and controlled manner.

Application of EGS in Sweden

Comparing different projects in different geological settings may be complex. However, in simple terms, granite was successfully stimulated and wells were connected with fluid flows of 30 l/s at 5 km in Soultz and 19 l/s at 4.1 km in Habanero. Fluid flow rates in United Downs are confidential, but >20 l/s may be assumed due to continued activity at the site. The main distinctions at these different locations relative to the geology of Sweden include:

- Higher geothermal gradients, probably due to thinner lithosphere and/or more heat producing RA elements.

- Tertiary deformation (extension in Soultz, compression in Habanero, and strike-slip faulting in United Downs). This event might also have caused more permeability and convective heating.

In Sweden, the last large deformation event, apart from the recent and current activity in the Tornqvist zone and faulting from glacial rebound, is from mid-Paleozoic Caledonian orogeny. However, earlier extensive deformation events acting on FSS have developed large shear zones with severe fracturing, hence fractures in all directions exists. The main question is whether the prevailing stress field is sufficient to assist hydro shearing and generate enough permeability at depth. To what extent did the glacial uplift reactivate shear zones in Sweden, and how does this affect the in-situ stress at depth and the fracture connectivity? For certain, in-situ stress measurements at depth would be useful, these measurements hasn't been found from any of the case projects in this study. Additionally, there is not yet enough information to determine the optimal stress regime for EGS development. The successful flow tests in United Downs reveal that a large strike-slip fault zone, perfectly aligned with the strike-slip stress field, is highly promising and raises a point regarding whether steeper dips are more suitable for a reservoir target at depth given the slightly lower lithostatic pressures acting on the reservoir due to assumed lower density of the more porous rocks forming the overburden. It might also require less fluid pressure to keep the sheared vertical structures open, for the same reason. In the United Downs project, the gravitational force also induce fluid flow downwards, which is especially true when the water is cold, i.e.- higher density. Despite the largely unknown details of the deformation structures in the FSS, especially at depth, an understanding of the tectonic history will increase the chances of more accurate conceptual models for the planning and well design of EGS projects in Sweden. Deep structures and their relationship to the surface is relevant, where long linear structures and topographic lows indicate shear zones. Sweden has good exposure due to glaciation revealing shear zones as topographic lows. However, these shear zones are naturally filled with till and other loose materials, making it difficult to see cataclasite, fault breccias and gauges, and/or oxidized surfaces.

A simplified pre-feasibility investigation of favorable EGS locations in Sweden would at the first stage suggest the heat anomaly in Småland (Figure 5). Assessing the geological map, long linear deformation structures (Figure 11) in line with the stress field, assuming a strike-slip regime at depth (Figure 12B) could be interpreted as second advantage. Furthermore, referring to Fouriers law (Geothermal gradient), the low thermal conductive sedimentary layers in Gotland, Öland and Skåne suggests higher geothermal gradients, where the most promising deformation structures to assist hydro shearing might be associated with the highly fractured Tornqvist-zone. The geothermal gradient of 22°C/km in the crystalline basement in Lund is also promising, especially if the thermal anomaly is not only due to high RA element concentrations, but also deep deformation structures which indicate permeable structures at depth. As shown in the geothermal plant in Lund, the support from electrical heat pumps should not be underestimated. For all Swedish previous EGS projects, the goal has been output temperatures of at least 100°C. However, it cost less energy to heat up 40-80 °C water to 100°C than from 10-20°C. A logical step in the process of utilizing the deep geothermal heat from crystalline rocks might be to start more shallow with heat pumps and use the learnings to go deeper, like they did in Soultz (page 24). When the next district heating generation emerges, these lower temperatures might be more attractive.

If the issues presented above are understood, coordinated, and optimized with realistic expectations, the possibility of successful EGS is considered promising in Sweden. It has only been tried once in a similar geological setting (in Espoo), hence the lessons from Espoo should provide opportunities for improvement. In this study, disregarding the promising and innovative drilling and modelling techniques, a better understanding of the crustal response to dynamic processes seems key to establish a successful EGS project in Sweden, and for that matter any place on Earth. Due to the unconventional nature of the FSS for deep geothermal energy extraction and the fact that each geological context is unique, a commercial EGS success would send a signal that deep geothermal energy now can be extracted almost everywhere on the planet.

Conclusions

A successful EGS project in Sweden requires connected open fracture systems at depth. This can be achieved through hydraulic stimulation. To enhance the possibility of doing this successfully, an understanding of deep brittle structures and their relation to the prevailing in-situ stress field and the tectonic regime is required. If fully understood, an optimal planning of the well geometries can be developed in order to obtain maximum fluid flow and reservoir size.

- As the experience from deep geothermal exploration accumulates, greater subsurface knowledge of rock stresses and connected fracture systems will be gained. This subsurface experience is shown to have a large impact on both the conceptual plan and the final EGS performance.
- In Sweden, the regional SHmax and the tectonic regime vary, as does the orientation of deformation structures. A suitable match of fractures aligned with the preferred orientation in relation to the tectonic regime most likely exists at depth in the extensively deformed Fennoscandian Shield.
- When a location for EGS is considered, the tectonic evolution of the surface structures should be investigated and understood using suitable geophysical methods, so that a subsurface interpretation of the structures can be used to develop a conceptual model with as high resolution as possible.
- Based on the drilling result from Espoo, the DTH technique seems to be highly appropriate for impermeable crystalline rocks, both to reduce drilling time and to making vertical seismic profiles (VSP) that follow structures while drilling.
- A VSP survey while drilling is recommended in order to follow the target with as much control as possible.
- To reduce the triggering of high magnitude earthquakes, a characterization and delineation of the zones intended to be stimulated is needed. All structures intended to be stimulated should be described in a Mohr diagram to control the stimulation. Therefore, in-situ stress measurements with orientations and magnitudes are preferred.

Examples of recommended future research

- Greater understanding about connected fracture systems at depth.
- Improved extrapolation of the stress field at depth from test-holes.
- Determination of the most suitable tectonic regime for induced permeability.
- Establish accurate geothermal gradients for determination of project feasibility. As more deep geothermal projects/deep boreholes accumulate, the more correlation between the subsurface, surface and geophysics can be established. These correlations will be useful in future feasibility studies.
- More studies like this, with more data, talking to more experts and quantify the lessons learned within a similar, well established EGS framework.

Acknowledgements

I have involved many people in this thesis whom all helped me in my understanding. A special thanks to my supervisor Victoria Pease who allowed me to execute this “made up” project. Extra thanks to Lasse Aman, introducing me to the world of drilling, giving me office space and many rewarding discussions. Maria Ask and Signhild Gehlin have helped me in the beginning and in the end. Vera Leier gave me ideas on how to organize the interviews. Also, all interview respondents and other people that helped me to come in contact with experts: M. Erlström, J. Rosberg, T. Arola, J. Hogmalm, T. Saarno, Y. Geraud, S. Park, K. Mallin, J. Andersson, U. Ring, J. Barth, P. Evins and A. Peillod .

References

Al-Darweesh, J., Aljawad, M. S., Al-Ramadan, M., Elkatatny, S., Mahmoud, M., & Patil, S. (2023). Review of underbalanced drilling techniques highlighting the advancement of foamed drilling fluids. *Journal of Petroleum Exploration and Production Technology*, *13*(4), 929–958. https://doi.org/10.1007/s13202-022-01596-w

Andersson, O. (1980). *Geotermisk värme till fjärrvärmenät i Vellinge*.

Artemieva, I. M., Thybo, H., Jakobsen, K., Sørensen, N. K., & Nielsen, L. S. K. (2017). Heat production in granitic rocks: Global analysis based on a new data compilation GRANITE2017. *Earth-Science Reviews*, *172*, 1–26. https://doi.org/10.1016/j.earscirev.2017.07.003

Baisch, S., Vörös, R., Rothert, E., Stang, H., Jung, R., & Schellschmidt, R. (2010). A numerical model for fluid injection induced seismicity at Soultz-sous-Forêts. *International Journal of Rock Mechanics and Mining Sciences*, *47*(3), 405–413. https://doi.org/10.1016/j.ijrmms.2009.10.001

Baltybaev, Sh. K. (2013). Svecofennian Orogen of the Fennoscandian Shield: Compositional and isotopic zoning and its tectonic interpretation. *Geotectonics*, *47*(6), 452–464. https://doi.org/10.1134/S0016852113060022

Barbier, E., & Fanelli, M. (1977). Non-electrical uses of Geothermal energy. *Progress in Energy and Combustion Science*, *3*(2), 73–103. https://doi.org/10.1016/0360-1285(77)90009-0

Baujard, C., Genter, A., Cuenot, N., Mouchot, J., Maurer, V., Hehn, R., Ravier, G., Seibel, O., & Vidal, J. (2018). *Experience Learnt from a Successful Soft Stimulation and Operational*

Feedback after 2 Years of Geothermal Power and Heat Production in Rittershoffen and Soultz-sous-Forêts Plants (Alsace, France). 12.

Baujard, C., Rolin, P., Dalmais, É., Hehn, R., & Genter, A. (2021). Soultz-sous-Forêts Geothermal Reservoir: Structural Model Update and Thermo-Hydraulic Numerical Simulations Based on Three Years of Operation Data. *Geosciences*, *11*(12), Article 12. https://doi.org/10.3390/geosciences11120502

Bertrand, L., Géraud, Y., & Diraison, M. (2021). Petrophysical properties in faulted basement rocks: Insights from outcropping analogues on the West European Rift shoulders. *Geothermics*, *95*, 102144. https://doi.org/10.1016/j.geothermics.2021.102144

Chang, K. W., Yoon, H., Kim, Y., & Lee, M. Y. (2020). Operational and geological controls of coupled poroelastic stressing and pore-pressure accumulation along faults: Induced earthquakes in Pohang, South Korea. *Scientific Reports*, *10*(1), Article 1. https://doi.org/10.1038/s41598-020-58881-z

Chinese Gov Announcement. (2021). *China Focus: China goes all out to pursue low-carbon growth—China.org.cn*. China Focus: China Goes All out to Pursue Low-Carbon Growth. http://www.china.org.cn/china/Off_the_Wire/2021-12/29/content_77959853.htm

Dalla Santa, G., Galgaro, A., Sassi, R., Cultrera, M., Scotton, P., Mueller, J., Bertermann, D., Mendrinos, D., Pasquali, R., Perego, R., Pera, S., Di Sipio, E., Cassiani, G., De Carli, M., & Bernardi, A. (2020). An updated ground thermal properties database for GSHP applications. *Geothermics*, *85*, 101758. https://doi.org/10.1016/j.geothermics.2019.101758

Davies, J. H., & Rhodri Davies, D. (2010). *Earth's Surface Heat Flux*. 3303. https://ui.adsabs.harvard.edu/abs/2010EGUGA..12.3303D

Deichmann, N., Kraft, T., & Evans, K. F. (2014). Identification of faults activated during the stimulation of the Basel geothermal project from cluster analysis and focal mechanisms of the larger magnitude events. *Geothermics*, *52*, 84–97. https://doi.org/10.1016/j.geothermics.2014.04.001

Dezayes, Ch. (2005). *Deep Geothermal Energy in Western Europe: The Soultz Project* (Public Document http://infoterre.brgm.fr/rapports/RP-54227-FR.pdf; p. 48). BRGM/RP-54227-FR. http://infoterre.brgm.fr/rapports/RP-54227-FR.pdf

Durst, P. (2013). *Overview of the Soultz geothermal project*. GEIE GMC presentation, Pisa, Italy.

Ellsworth, W. L. (2019). Triggering of the Pohang, Korea, earthquake (M w 5.5) by enhanced geothermal system stimulation. *Seismological Research Letters*, *90(5)*, 1844–1858. https://doi-org.ezp.sub.su.se/10.1785/0220190102

Energimyndigheten. (2021). *Demonstration av testhål för utveckling av Engineered Geothermal Systems*.

Energimyndigheten. (2023). Energiläget 2022—Med energibalanser för år 1970-2020. *Energiläget*, *2022*, 103.

Fang-chao K., Chun-an T., Ying-chun L. I., Tian-jiao L. I., & Jin-long M. E. N. (2022). Challenges and opportunities of enhanced geothermal systems: A review. 工程科学学报, *44*(10), 1767–1777. https://doi.org/10.13374/j.issn2095-9389.2022.04.07.004

Farndale, H., & Law, R. (2022). An Update on the United Downs Geothermal Power Project, Cornwall, UK. *P ROCEEDINGS, 47th Workshop on Geothermal Reservoir Engineering*, *47*, 13.

Finger, J., & Blankenship, D. (2012). *Handbook of Best Practices for Geothermal Drilling* (No. SAND2011--6478, 1325261, 587569; pp. SAND2011--6478, 1325261, 587569). https://doi.org/10.2172/1325261

Fridleifsson, G. O., Bogason, S. G., Stoklosa, A. W., Ingolfsson, H. P., Vergnes, P., Thorbjörnsson, I. Ö., Peter-Borie, M., Kohl, T., Edelmann, T., & Bertani, R. (2016). *DEPLOYMENT OF DEEP ENHANCED GEOTHERMAL SYSTEMS FOR SUSTAINABLE ENERGY BUSINESS*.

Furlong, K. P., & Chapman, D. S. (2013). Heat Flow, Heat Generation, and the Thermal State of the Lithosphere. *Annual Review of Earth and Planetary Sciences*, *41*(1), 385–410. https://doi.org/10.1146/annurev.earth.031208.100051

Gehlin, S., Andersson, O., & Rosberg, J.-E. (2020). Country Update for Sweden 2020. *World Geothermal Congress 2020+1*, *2020*, 9.

Gischig, V., & Preisig, G. (2015). *HYDRO-FRACTURING VERSUS HYDRO-SHEARING: A CRITICAL ASSESSMENT OF TWO DISTINCT RESERVOIR STIMULATION MECHANISMS*. https://doi.org/10.13140/RG.2.1.4924.3041

Häring, M. O. (2004). Deep Heat Mining: Development of a Cogeneration Power Plant from an Enhanced Geothermal System in Basel, Switzerland. *Geothermal Resources Council Transactions*, *28*.

Häring, M. O. (2008). *Lessons Learnt from the Deep Heat Mining EGS Project in Basel, Switzerland* [Presentation]. Australian Geothermal Energy Conference 2008, Australia. https://www.geothermal-energy.org/pdf/IGAstandard/AGEC/2008/Haring_et_al_2008.pdf

Häring, M. O., Schanz, U., Ladner, F., & Dyer, B. C. (2008). Characterisation of the Basel 1 enhanced geothermal system. *Geothermics*, *37*(5), 469–495. https://doi.org/10.1016/j.geothermics.2008.06.002

Heikkinen, P., Giese, R., & Kukkonen, I. (2021). Basement-EGS Structure from VSP, Drilling, Well Logs, and Geology in Espoo, Finland. *GRC Transactions*, *45*(2021). https://publications.mygeoenergynow.org/grc/1034472.pdf

Heller, R., Duda, J.-P., Winkler, M., Reitner, J., & Gizon, L. (2021). Habitability of the early Earth: Liquid water under a faint young Sun facilitated by strong tidal heating due to a closer Moon. *PalZ*, *95*(4), 563–575. https://doi.org/10.1007/s12542-021-00582-7

Henkel, H. (2007). Slutrappport avseende geovetenskapliga undersökningar. *MSc Thesis*. https://www.academia.edu/28471074/Slutrappport_avseende_geovetenskapliga_unders%C3%B6kningar

Henkel, H., & Guzmán, M. (1977). Magnetic features of fracture zones. *Geoexploration*, *15*(3), 173–181. https://doi.org/10.1016/0016-7142(77)90024-2

Hogarth, R., & Holl, H.-G. (2017a). Lessons learned from the Habanero EGS project. *Transactions - Geothermal Resources Council*, *41*.

Hogarth, R., & Holl, H.-G. (2017b). Lessons Learned from the Habanero EGS Project. *GRC Transactions*, *41*, 13.

Hogmalm, J., Tillberg, M., & Angelbratt, A. (2021). *GE-1 DRILLING – GEOLOGICAL REPORT* [Internal report]. Göteborgs Energi.

Holmgren, J. M., Kwiatek, G., & Werner, M. J. (2023). Nonsystematic Rupture Directivity of Geothermal Energy Induced Microseismicity in Helsinki, Finland. *Journal of Geophysical Research: Solid Earth*, *128*(3), e2022JB025226. https://doi.org/10.1029/2022JB025226

Hoseini, E. (2007). *Värmeflödet från jordens inre och dess användning som energikälla* [MSc thesis, LTU]. http://www.diva-portal.org/smash/get/diva2:1029999/FULLTEXT01.pdf

Humphreys, B. (2014). *Habanero Geothermal Project Field Development Plan.pdf*. Geodynamics Limited. https://arena.gov.au/assets/2016/10/Habanero-Geothermal-Project-Field-Development-Plan.pdf

Ingebritsen, S. e., & Manning, C. E. (1999). Geological implications of a permeability-depth curve for the continental crust. *Geology*, *27*(12), 1107. https://doi.org/10.1130/0091-7613(1999)027<1107:GIOAPD>2.3.CO;2

Ito, T., & Zoback, M. D. (2000). Fracture permeability and in situ stress to 7 km depth in the KTB scientific drillhole. *Geophysical Research Letters*, *27*(7), 1045–1048. https://doi.org/10.1029/1999GL011068

Jia, Y., Tsang, C.-F., Hammar, A., & Niemi, A. (2022). Hydraulic stimulation strategies in enhanced geothermal systems (EGS): A review. *Geomechanics and Geophysics for Geo-Energy and Geo-Resources*, *8*(6), 211. https://doi.org/10.1007/s40948-022-00516-w

Juhlin, C., Erlström, M., Lund, B., & Rosberg, J.-E. (2022). Seismic reflectivity, fracturing and stress field data from the FFC-1 exploratory geothermal project in SW Skåne, Sweden. *Geothermics*, *105*, 102521. https://doi.org/10.1016/j.geothermics.2022.102521

Karlsson, P.-A. (2022, May 5). *Geotermi – erfarenheter av DjupGeo och tankar om framtiden* [ST1 Presentation].

Kervall, H. (2021). *Feasibility of Enhanced Geothermal Systems in the Precambrian crystalline basement in SW Scania, Sweden* [MSc thesis]. Lund University.

Kim, H. C., & Lee, Y. (2007). Heat flow in the Republic of Korea. *Journal of Geophysical Research*, *112*(B5), B05413. https://doi.org/10.1029/2006JB004266

Kölbel, T., & Genter, A. (2017). *Enhanced Geothermal Systems: The Soultz-sous-Forêts Project* (pp. 243–248). https://doi.org/10.1007/978-3-319-45659-1_25

Kraft, T., Mai, P., Wiemer, S., Deichmann, N., Ripperger, J., Kästli, P., Layland-Bachmann, C., Fäh, D., Woessner, J., & Giardini, D. (2009, December 1). *Enhanced Geothermal Systems in Urban Areas—Lessons Learned from the 2006 Basel ML3.4 Earthquake*. AGU Fall Meeting Abstracts.

Kukkonen, Heikkinen, P. J., Malin, P. E., Renner, J., Dresen, G., Karjalainen, A., Rytkönen, J., & Solantie, J. (2023). Hydraulic conductivity of the crystalline crust: Insights from hydraulic stimulation and induced seismicity of an enhanced geothermal system pilot reservoir at 6 km depth, Espoo, southern Finland. *Geothermics*, *112*, 102743. https://doi.org/10.1016/j.geothermics.2023.102743

Kukkonen, I. (1989). *Terrestrial heat flow in Finland, the central Fennoscandian Shield* [PhD thesis]. Geological Survey of Finland.

Kukkonen, I. T., & Pentti, M. (2021). St1 Deep Heat Project: Geothermal energy to the district heating network in Espoo. *IOP Conference Series: Earth and Environmental Science*, *703*(1), 012035. https://doi.org/10.1088/1755-1315/703/1/012035

Kwiatek, G., Saarno, T., Ader, T., Bluemle, F., Bohnhoff, M., Chendorain, M., Dresen, G., Heikkinen, P., Kukkonen, I., Leary, P., Leonhardt, M., Malin, P., Martínez-Garzón, P., Passmore, K., Passmore, P., Valenzuela, S., & Wollin, C. (2019). Controlling fluid-induced seismicity during a 6.1-km-deep geothermal stimulation in Finland. *Science Advances*, *5*(5), eaav7224. https://doi.org/10.1126/sciadv.aav7224

Le Boutillier, N. (2002). *The Tectonics of Variscan Magmatism and Mineralisation in South West England—Volume II*. https://doi.org/10.13140/RG.2.2.21395.68642

Ledingham, P., Cotton, L., & Law, R. (2019). The United Downs Deep Geothermal Power Project. *44th Workshop on Geothermal Reservoir Engineering*, *44th*.

Lee, T. J., Song, Y., Park, D.-W., Jeon, J., & Yoon, W. S. (2015). Three Dimensional Geological Model of Pohang EGS Pilot Site, Korea. *Proceedings World Geothermal Congress, Melbourne, Australia, 19-25 April 2015*.

Leonhardt, M., Kwiatek, G., Martínez-Garzón, P., Bohnhoff, M., Saarno, T., Heikkinen, P., & Dresen, G. (2021). Seismicity during and after stimulation of a 6.1 km deep enhanced geothermal system in Helsinki, Finland. *Solid Earth*, *12*(3), 581–594. https://doi.org/10.5194/se-12-581-2021

Li, S., Wang, S., & Tang, H. (2022). Stimulation mechanism and design of enhanced geothermal systems: A comprehensive review. *Renewable and Sustainable Energy Reviews*, *155*, 111914. https://doi.org/10.1016/j.rser.2021.111914

Lim, H., Deng, K., Kim, Y. h., Ree, J.-H., Song, T.-R. A., & Kim, K.-H. (2020). The 2017 Mw 5.5 Pohang Earthquake, South Korea, and Poroelastic Stress Changes Associated With Fluid Injection. *Journal of Geophysical Research: Solid Earth*, *125*(6), e2019JB019134. https://doi.org/10.1029/2019JB019134

Lorenz, H., Rosberg, J.-E., Juhlin, C., Bjelm, L., Almqvist, B., Berthet, T., Conze, R., Gee, D., Klonowska, I., Pascal, C., Pedersen, K., Roberts, N., & Tsang, C.-F. (2015). COSC-1 – drilling of a subduction-related allochthon in the Palaeozoic Caledonide orogen of Scandinavia. *Scientific Drilling*, *19*, 1–11. https://doi.org/10.5194/sd-19-1-2015

Lundqvist, J. (2011). *Sveriges geologi från urtid till nutid* (3rd ed.). Studentlitteratur. https://www.adlibris.com/se/bok/sveriges-geologi-fran-urtid-till-nutid-9789144058474

Malek, A. E., Adams, B. M., Rossi, E., Schiegg, H. O., & Saar, M. O. (2022). Techno-economic analysis of Advanced Geothermal Systems (AGS). *Renewable Energy*, *186*, 927–943. https://doi.org/10.1016/j.renene.2022.01.012

Manzella, A. (2016). *The Role of Magnetotellurics in Geothermal Exploration* [CNR - Institute of Geosciences and Earth Resources]. National Research Council of Italy, Pisa. https://www.dias.ie/wp-content/uploads/2016/07/Session3_AManzella_Iretherm2016.pdf

McGarr, A. (2023). The 2017 Pohang, South Korea, Mw 5.4 main shock was either natural or triggered, but not induced. *Geothermics*, *107*(102612). https://doi.org/10.1016/j.geothermics.2022.102612

McIntire,P.E., Mills,A.L. and G.M.Hornberger 1988. Interactions between groundwater seepage and sediment porewater sulfate concentration profiles in Lake Anna, Virginia. Hydrol. Proc., 2:207 217.

Meyer, B., Lacassin, R., Brulhet, J., & Mouroux, B. (2007). The Basel 1356 earthquake: Which fault produced it? *Terra Nova*, *6*, 54–63. https://doi.org/10.1111/j.1365-3121.1994.tb00633.x

Moeck, I. S. (2014). Catalog of geothermal play types based on geologic controls. *Renewable and Sustainable Energy Reviews*, *37*, 867–882. https://doi.org/10.1016/j.rser.2014.05.032

Naik, S. P., Gwon, O., Porfido, S., Park, K., Jin, K., Kim, Y.-S., & Kyung, J.-B. (2020). Intensity Reassessment of the 2017 Pohang Earthquake Mw = 5.4 (South Korea) Using ESI-07 Scale. *Geosciences*, *10*(11), Article 11. https://doi.org/10.3390/geosciences10110471

Naturvårdsverket. (2022). *Import och export av avfall*. Naturvårdsverket. https://www.naturvardsverket.se/data-och-statistik/avfall/avfall-import-export

OECD/IEA. (2011). *Technology roadmap: Geothermal heat and power.* Renewable Energy Division, International Energy Agency.

Olsson, L., Wetterlund, E., & Söderström, M. (2015). Assessing the climate impact of district heating systems with combined heat and power production and industrial excess heat. *Resources, Conservation and Recycling*, *96*, 31–39. https://doi.org/10.1016/j.resconrec.2015.01.006

Ozgener, L., Hepbasli, A., & Dincer, I. (2007). A key review on performance improvement aspects of geothermal district heating systems and applications. *Renewable and Sustainable Energy Reviews*, *11*(8), 1675–1697. https://doi.org/10.1016/j.rser.2006.03.006

Park, S., Kim, K.-I., Xie, L., Yoo, H., Min, K.-B., Kim, M., Yoon, B., Kim, K. Y., Zimmermann, G., Guinot, F., & Meier, P. (2020). Observations and analyses of the first two hydraulic stimulations in the Pohang geothermal development site, South Korea. *Geothermics*, *88*, 101905. https://doi.org/10.1016/j.geothermics.2020.101905

Parker, R. (1999). The Rosemanowes HDR project 1983–1991. *Geothermics*, *28*(4), 603–615. https://doi.org/10.1016/S0375-6505(99)00031-0

Place, J., Diraison, M., Géraud, Y., & Koyi, H. A. (2018). Horst Inversion Within a Décollement Zone During Extension Upper Rhine Graben, France. In A. A. Misra & S. Mukherjee (Eds.), *Atlas of Structural Geological Interpretation from Seismic Images* (pp. 47–49). John Wiley & Sons, Ltd. https://doi.org/10.1002/9781119158332.ch7

Place, J., Sausse, J., Marthelot, J.-M., Diraison, M., Géraud, Y., & Naville, C. (2011). 3-D mapping of permeable structures affecting a deep granite basement using isotropic 3C VSP data: Mapping structures in a deep granite basement. *Geophysical Journal International*, *186*(1), 245–263. https://doi.org/10.1111/j.1365-246X.2011.05012.x

Pratiwi, A., Ravier, G., & Genter, A. (2018). Life-cycle climate-change impact assessment of enhanced geothermal system plants in the Upper Rhine Valley. *Geothermics*, *75*, 26–39. https://doi.org/10.1016/j.geothermics.2018.03.012

Quaise Energy. (2023). Quaise Energy. https://www.quaise.energy/

Reinecker, J. (2021). *United Downs Deep Geothermal Project, UK* [Presentation].

Reinecker, J., Gutmanis, J., Foxford, A., Cotton, L., Dalby, C., & Law, R. (2021). Geothermal exploration and reservoir modelling of the United Downs deep geothermal project, Cornwall (UK). *Geothermics*, *97*, 102226. https://doi.org/10.1016/j.geothermics.2021.102226

Rodríguez-Pradilla, G., & Verdon, J. (2021). *Seismic Monitoring of the United Downs Deep Geothermal Power Project (UDDGP) Site with Public Seismic Networks*. *2021*(1), 1–5. https://doi.org/10.3997/2214-4609.202113053

Rosberg, J.-E., & Erlström, M. (2019). Evaluation of the Lund deep geothermal exploration project in the Romeleåsen Fault Zone, South Sweden: A case study. *Geothermal Energy*, *7*(1), 10. https://doi.org/10.1186/s40517-019-0126-7

Rosberg, J.-E., & Erlström, M. (2021). Evaluation of deep geothermal exploration drillings in the crystalline basement of the Fennoscandian Shield Border Zone in south Sweden. *Geothermal Energy*, *9*(1), 20. https://doi.org/10.1186/s40517-021-00203-1

Rosener, M., & Géraud, Y. (2007). Using physical properties to understand the porosity network geometry evolution in gradually altered granites in damage zones.

Geological Society, London, Special Publications, *284*(1), 175–184. https://doi.org/10.1144/SP284.12

Röth, J., & Littke, R. (2022). Down under and under Cover—The Tectonic and Thermal History of the Cooper and Central Eromanga Basins (Central Eastern Australia). *Geosciences*, *12*(3), Article 3. https://doi.org/10.3390/geosciences12030117

Rychert, C. A., Harmon, N., Constable, S., & Wang, S. (2020). The Nature of the Lithosphere-Asthenosphere Boundary. *Journal of Geophysical Research: Solid Earth*, *125*(10), e2018JB016463. https://doi.org/10.1029/2018JB016463

Slagstad, T., Balling, N., Elvebakk, H., Midttømme, K., Olesen, O., Olsen, L., & Pascal, C. (2009). Heat-flow measurements in Late Palaeoproterozoic to Permian geological provinces in south and central Norway and a new heat-flow map of Fennoscandia and the Norwegian–Greenland Sea. *Tectonophysics*, *473*(3–4), 341–361.

Steffen, H., Olesen, O., & Sutinen, R. (Eds.). (2021). Modelling of Glacially Induced Faults and Stress. In *Glacially-Triggered Faulting* (1st ed., pp. 381–416). Cambridge University Press. https://doi.org/10.1017/9781108779906.028

Stephansson. (1988). Ridge Push Glacial Rebound Rock Stress Generators Fennoscandian Shield. *Bulletin of the Geological Institutions on the University of Uppsala*, *14*(1988), 39-48.

Stober, I., Ladner, F., Hofer, M., & Bucher, K. (2022). The deep Basel-1 geothermal well: An attempt assessing the predrilling hydraulic and hydrochemical conditions in the basement of the Upper Rhine Graben. *Swiss Journal of Geosciences*, *115*(1), 3. https://doi.org/10.1186/s00015-021-00403-8

Swiss Seismological Service. (2017). *SED | Geothermal Energy Basel*. Project Description Geothermal Energy Basel. http://www.seismo.ethz.ch/en/earthquakes/monitoring/special-networks/basel/

Tammemagi, H. Y., & Wheildon, J. (1977). Further data on the South-west England heat flow anomaly. *Geophysical Journal International*, *49*(2), 531–539. https://doi.org/10.1111/j.1365-246X.1977.tb03721.x

Tester, W. (Ed.). (2006). *The future of geothermal energy: Impact of enhanced geothermal systems (EGS) on the United States in the 21st century: an assessment*. Massachusetts Institute of Technology.

Todd, K. (1980). *Groundwater Hydrology*. Wiley.

Ulutaş, E. (2020). The May 11 Paphos, Cyprus, earthquake: Implications for stress regime and tsunami modelling for the Eastern Mediterranean shorelines. *Arabian Journal of Geosciences*, *13*, 970. https://doi.org/10.1007/s12517-020-05943-1

Uski, M., Hyvönen, T., Korja, A., & Airo, M.-L. (2003). Focal mechanisms of three earthquakes in Finland and their relation to surface faults. *Tectonophysics*, *363*(1), 141–157. https://doi.org/10.1016/S0040-1951(02)00669-8

Ustaszewski, K., & Schmid, S. M. (2007). Latest Pliocene to recent thick-skinned tectonics at the Upper Rhine Graben – Jura Mountains junction. *Swiss Journal of Geosciences*, *100*(2), Article 2. https://doi.org/10.1007/s00015-007-1226-0

Veikkolainen, T., Kukkonen, I., & Tiira, T. (2017). Heat flow, seismic cutoff depth and thermal modeling of the Fennoscandian Shield. *Geophysical Journal International*, *211*, 1414–1427. https://doi.org/10.1093/gji/ggx373

Wahlgren, C.-H., Schoning, K., Tenne, M., & Hansen, L. M. (2019). The geological evolution of Stockholm – bedrock, Quaternary deposits and experience from infrastructure projects. *SGU Report*.

Wahlström, R. (1993). Fennoscandian seismicity and its relation to the isostatic rebound. *Global and Planetary Change*, *8*(3), 107–112. https://doi.org/10.1016/0921-8181(93)90018-J

Wallroth, T., Eliasson, T., & Sundquist, U. (1999). *Hot dry rock research experiments at FjaÈ llbacka, Sweden*. 9.

Warr, L. N., Primmer, T. J., & Robinson, D. (1991). Variscan very low-grade metamorphism in southwest England: A diastathermal and thrust-related origin. *Journal of Metamorphic Geology*, *9*(6), 751–764. https://doi.org/10.1111/j.1525-1314.1991.tb00563.x

Werner, S. (2017). District heating and cooling in Sweden. *Energy*, *126*, 419–429. https://doi.org/10.1016/j.energy.2017.03.052

Wisian, K. W., & Blackwell, D. D. (2004). Numerical modeling of Basin and Range geothermal systems. *Geothermics*, *33*(6), 713–741. https://doi.org/10.1016/j.geothermics.2004.01.002

Wyborn, D. (2010). Update of Development of the Geothermal Field in the Granite at Innamincka, South Australia. *Proceedings World Geothermal Congress 2010*, *Bali, Indonesia*. https://www.geothermal-energy.org/pdf/IGAstandard/WGC/2010/3121.pdf

Zheng, X. (2023, May). China begins drilling of ultra-deep oil well in Tarim Basin. *China Daily*. https://www.chinadaily.com.cn/a/202305/30/WS6475e8dca310b6054fad5d69.html

Ziegler, M., Valley, B., & Evans, K. (2015, April 1). *Characterisation of Natural Fractures and Fracture Zones of the Basel EGS Reservoir inferred from Geophysical Logging of the Basel-1 Well*.

Appendix

A1

Letter of Intent

Elof Tehler
Telephone: +46 708 696 212
Email: elof.tehler@gmail.com
(supervisor: Prof. Victoria Pease,
email: Vicky.pease@geo.su.se)

Stockholms universitet

Title of Project: Deep geothermal energy extraction in Sweden? Case study based on interviews and a literature review from 6 EGS projects

Information Sheet for respondents

Dear respondent,

I am a Master's of Science student in geology. My field of interest is structural geology applied geology, with geothermal energy as a special interest. In this master thesis, I will evaluate the most important geological and operational parameters for future deep geothermal energy exploration projects in Sweden.

Unconventional geothermal resource?
Since the Swedish bedrock is composed of the crystalline Fennoscandian Shield (FSS), this study assumes that rocks at depth are impermeable and therefore require hydro shearing for induced fluid flow, often referred to as EGS (enhanced geothermal system). I also assume the geothermal gradient is low, between 16-22°C/km, requiring deep geothermal reservoirs to obtain high temperatures.

Most EGS projects that has been carried out so far aim for electricity production, requiring bottom-hole temperatures (BHT) of a minimum 150°C. The subarctic-to-temperate climate in Sweden creates a great demand for heating. In most Swedish urban areas, district heating networks are well developed. Most heating of households and factories comes from district heating. The district heating production comes mainly from the burning of biofuels from forestry and waste. If geothermal heat acted as a district heating producer, it would cut transportation costs and erase the environmental disadvantage associated with the incineration process. The geological setting of Sweden is usually considered geothermally non-conventional since it's sitting on the old, thick, cold and tectonically inactive FSS. However, since the final goal is water heating for district heating systems, there is no need for costly electricity conversions and therefore, lower BTHs might be sufficient. By combining the geological setting of Sweden with a review of the basic principles behind EGS and 6 EGS projects that have been carried out, I hope to contribute with insights into the most important geological and operational parameters.

To increase my chances of making a credible assessment of each EGS project, I will interview at least one expert from each EGS project. Each interview will be semi-structured, and take maximum 45 minutes and the respondent will receive an agenda to get prepared at least two days before the interview. The EGS projects that will be evaluated are:

- Soultz, Basel, Habanero, Pohang, United Downs and Espoo.

I would like to invite you to participate in this study!

If you are interested in taking part in this research, you are asked to give information about your learning experiences and your particular viewpoints during our interview. The interview will be recorded and transcribed and will be conducted by the MSc thesis author (Elof Tehler). In the interview you will be asked about your experience, knowledge and opinions related to my research topic as described above. Participation in this study is voluntary, and you have the right to withdraw from the study at any stage. If you withdraw, I will do my best to remove any information relating to you, provided this is practically achievable.

Please be assured that particular care will be taken to ensure the confidentiality of all reseach data gathered for this study. The data will be held securely by the researcher and kept for a period of 1 year and will be destroyed after that..

This study may be used for publication in national and international journals, and the outcomes may be presented at national and international conferences. I would like to offer you a copy of the report and/or a summary of the findings. You may ask for additional information or results from the study at any time.

If you choose to participate, I would appreciate it if you would return the signed consent form to me by email by 31 May 2023.

If you have any questions about this research, please do not hesitate to contact me or my supervisor. Details are at the top of this letter.

Thank you for considering taking part in this research.

Signature: XXX

_____

A2

Transcript example from interview

ET - 36:27,960;36:35,920;If you think about the Swedish perspective, the Fennoscandian is old and cold and thick lithosphere, how would you trace the most promising permeable zones at that depth?

XX - 36:50,240;37:00,280;"Oh, mostly. Maybe I think we must understand, where are the big fault systems and where are the more reactivated fault systems because we have a high discharge of the system, and you have some reactivation of some fault and now the regime. Yeah, from even ice retreating.

ET - 37:18,960;37:26,880;"Yes, ok

XX - 37:26,880;37:32,160;"We can have some reactivations too and maybe we can consider that that's an active fault system. Yeah, and this active fault system is probably a fault system where the permeability could be increased by the formation of fractures."

XX - 37:52,600;38:00,480;"And maybe open fractures because when you discharge, you decrease ice from the shield. We have an extension of processes we can develop on some faults. And maybe it could be a good target for that."

ET - 38:09,360;38:13,360;"Yeah, I think that too. These faults are only described in the north. But at least when I think about it, the ice were further south about ten thousand years ago. So it might be traces from that potential reactivation and more horizontal stress in the rocks even more south. To me that seems logic, but maybe stress is all released now"

XX - 38:42,560;38:50,960;"Yeah, but the other problem is that what is the depth that these faults could be, could be reactivated from this regime. Maybe it could be an important point and maybe it could be interesting to have some the VSP images because I think we can see this effect of at depth. The other point we can imagine to use the geothermal aspect in this kind of geological context. It's a new concept developed by an American company to have a continuous drilling from an injection point we have a very opaque depth and after we can move up to the surfaces and we can throw some feed inside this pipe and we can extract the heat from the depths part and without the natural permeability network because you are building your own permeability concrete."

ET - 40:09,200;40:14,480;"Yeah that's what they call advanced geothermal systems. Yeah but the critical people say that now it's not the volume is just not sufficient, it must be more water in contact with the warm rocks.

XX - 40:23,920;40:32,720; Yes thats clear. And the main problem is what we can do at depth to control the borehole geometry and to try to have this kind of tube at depth to extract the state. But I think technologically we can increase this capability to control what is the pathway for the 3D machine to have that time to have this kind of system developed in this kind of geological context.

ET - 40:57,040;41:02,480;"So finally I know time ends here. Are you okay with two three more minutes?"

XX - 41:02,480;41:08,400;"Yes